Karst Geology of Aguijan and Tinian, CNMI
Cave Inventory and Structural Analysis of Development

Kevin W. Stafford, John E. Mylroie & John W. Jenson

Department of Geosciences
Mississippi State University
Mississippi State, MS 39762

Water and Environmental Research Institute of the Western Pacific
University of Guam
Mangilao, Guam 96923

Technical Report No. 106

Water & Environmental Research Institute of the Western Pacific
University of Guam

September, 2004

WERI
WATER AND ENERGY RESEARCH INSTITUTE
OF THE WESTERN PACIFIC
UNIVERSITY OF GUAM

Karst Geology of Aguijan and Tinian, CNMI
Cave Inventory and
Structural Analysis of Development

Kevin W. Stafford, John E. Mylroie
& John W. Jenson

Department of Geosciences
Mississippi State University
Mississippi State, MS 39762

Water and Environmental Research Institute
of the Western Pacific
University of Guam
Mangilao, Guam 96923

Technical Report No. 106

Water & Environmental Research Institute
of the Western Pacific
University of Guam

September, 2004

THE WATER RESOURCES RESEARCH INSTITUTE PROGRAM OF THE US GEOLOGICAL SURVEY, AWARD NO. 01HQPA0010, SUPPORTED THE WORK REPORTED HERE. THE CONTENT OF THIS REPORT DOES NOT NECESSARILY REFLECT THE VIEWS AND POLICIES OF THE DEPPARTMENT OF THE INTERIOR, NOR DOES THE MENTION OF TRADE NAMES OR COMMERCIAL PRODUCTS CONSTITUTE THEIR ENDORSEMENT BY THE UNITED STATES GOVERNMENT.

ABSTRACT

Tinian and Aguijan, Commonwealth of the Northern Mariana Islands (CNMI), are volcanic, back arc islands in the western Pacific formed by Pacific Plate subduction under the Philippine Plate. The islands are composed of Eocene volcanic cores mantled by Plio-Pleistocene carbonate facies and raised Holocene beach and reef deposits. The entire sequence has been tectonically uplifted and contains high-angle normal faults, while isostatic subsidence and scarp failures overprint tectonic brittle failure features.

A cave and karst inventory on Tinian and Aguijan surveyed 114 features and is believed to adequately represent the megaporosity (cave) development. Two distinct cave classes were identified: mixing zone caves (flank margin caves and banana holes) and fissure caves. Most mixing zone caves were located in or near scarps and coastlines, often at similar elevations to nearby caves. Fissure caves were located in regions of brittle failure, forming linear features with narrow widths. Three previous sea-level positions were identified based on horizons of mixing zone caves. Seventeen freshwater discharge sites and four allogenic recharge sites were identified on Tinian.

Kolmogorov-Smirnov statistical analyses and rose diagram comparisons of orientation trends found significant similarities between megaporosity and geologic structure (brittle failure) on Tinian. Analyses of small regions showed distinct relations between brittle deformation and megaporosity, while at larger scales similarities became less obvious due to the complex geologic history and physiography of the island. Based on similarities in populations of orientation trends, fissure cave development is primarily controlled by brittle failure deformation with development along faults, fractures, and joints, while mixing zone cave development is primarily controlled by fresh-water lens position but significantly influenced by brittle failure deformation.

Tinian and Aguijan do not fit neatly into one classification of the Carbonate Island Karst Model. Regions of Tinian best fit the Simple, Carbonate-Cover and Composite Island Karst Models, but none easily fit the entire island. Aguijan must be classified as a Simple Carbonate Island because no geologic data has proved the presence of non-carbonate rocks interfering with the fresh-water lens, however it is probable that Aguijan does contain basement rocks that extend above sea-level as on other carbonate islands in the Marianas.

PREFACE

WERI (Water and Environmental Institute of the Western Pacific) Tech Report #96 was published as a preliminary assessment of the karst development and water resources of Tinian and Rota, CNMI (Commonwealth of the Northern Mariana Islands), based on a field reconnaissance conducted on the islands in June 2002. Since that time, work in the CNMI has focused on the Islands of Aguijan, Rota and Tinian with a primary emphasis on the cave and karst inventories of these islands, which can be used to evaluate the hydrolgeologic evolution of the islands.

The work presented in this study provides a detailed cave and karst inventory of the Islands of Aguijan and Tinian, CNMI with an analysis of structural controls on cave and karst development on the island of Tinian. The authors conducted this work as thesis research at Mississippi State University in conjunction with the University of Guam, while the US Geological Survey, through the National Institutes for Water Resources Research program, award no. 01HQGR0134, funded fieldwork. The data and findings in this report were originally published as a master's thesis by Kevin Stafford, titled: *Structural Controls on Megaporosity in Eogenetic Carbonate Rocks: Tinian, CNMI*. Ultimately, the work presented herein was made possible through the support of the Municipality of Tinian and Aguijan through: Tinian Mayors Office, CNMI Department of Land and Natural Resources, CNMI Department of Historical Preservation, Commonwealth Utilities Corporation, and Northern Marianas College.

Due to the large volume of data in this report, the appendices (Appendix A: Color Figures; Appendix B: Cave and Karst Inventory; Appendix C: Orientation Data; and Appendix D: Statistical Comparisons) are published as *.pdf* files in the attached CD or can be downloaded from the WERI website (www.uog.edu/weri). These appendices include color images of significant features, detailed maps of the inventoried karst features on Aguijan and Tinian, diagrams representing the structural geology of Tinian, and data matrices of statistical analyses.

Additional research continues in the Mariana Islands, in order to further answer questions about the karst geology and water resources of the islands. A similar study to the work reported herein is currently underway by the authors and master's thesis research by T. Montgomery Keel at Mississippi State University. Ultimately this study and future studies will be used to evaluate the fresh-water lens development on carbonate islands, which can be used to better manage the water resources of these communities.

CONTENTS

CONTENTS (cont.)

LIST OF TABLES

LIST OF FIGURES

LIST OF FIGURES (cont.)

LIST OF FIGURES (cont.)

LIST OF FIGURES (cont.)

LIST OF FIGURES (cont.)

KARST GEOLOGY OF AGUIJAN AND TINIAN, CNMI
Cave Inventory and Structural Analysis of Development

INTRODUCTION

This study has three primary objectives: 1) conduct a cave and karst inventory on Tinian and Aguijan, because no inventory existed, 2) investigate the cave and karst development on Tinian to determine if influences on mega-porosity development are associated with brittle deformation in eogenetic rocks, and 3) evaluate of the islands of Tinian and Aguijan in relation to the Carbonate Island Karst Model (Jenson et al., 2002; Mylroie and Jenson, 2002), in order to further advance the understanding of eogenetic karst development on carbonate islands.

The Tinian municipality of the Commonwealth of the Northern Mariana Islands (CNMI) governs Tinian and Aguijan. The Mariana Islands are a volcanic, back arc island chain in the western Pacific formed by Pacific Plate subduction under the Philippine Plate along the Mariana Trench. Aguijan covers 7.2 square kilometers and Tinian covers 102 square kilometers. A geologic study was conducted on Tinian in 1960 (Doan et al., 1960), which described the island as an Eocene volcanic core mantled by Plio-Pleistocene coralliferous and algal carbonate facies and raised Holocene beach and reef deposits. The entire sequence has been uplifted and contains high-angle normal faults produced from arc tectonism. Tinian has experienced greater than 100 meters of uplift since the Pleistocene, with an estimated 1.8 meters of uplift in the Holocene (Dickenson, 1999). Aguijan has only been studied briefly (Tayama, 1936) and no geologic map has been produced for the island; however, it is presumed to have a depositional and tectonic history similar to Tinian based on its proximity (~9 kilometers southwest of Tinian).

The Carbonate Island Karst Model predicts cave and karst development in eogenetic limestone (Jenson et al., 2002; Mylroie and Jenson, 2002; Mylroie and Jenson, 2001). It provides a fundamental and systematic framework for describing hydrogeologic karst evolution in young carbonate rocks, by incorporating the effects of mixing zone dissolution, glacio-eustacy, tectonism, and lithologic variations. In this model distinctive cave morphologies develop as eogenetic karst. These distinctive morphologies include flank margin caves, banana holes, pit caves, and stream caves. Traditionally, the affects of structural and lithologic controls on eogenetic karst development have been greatly overlooked because the original model was developed to describe features observed in the structurally and lithologically simple islands of the Bahamas (Mylroie and Carew, 1995a).

Structural control of karst development is common in continental settings, where the rock exhibits low porosity and is highly fractured (Klimchouk and Ford, 2000). Eogenetic karst is generally associated with caves formed by mixing zone dissolution, primarily independent of structural controls, in rocks that have never been buried beyond the range of meteoric diagenesis and retain high primary and syngenetic porosities. Recently, Jenson and coworkers (2002) recognized the importance of structural and lithologic controls on carbonate island karst and modified the Carbonate Island Karst Model to account for the effects of deformation and lithology on dissolution that occurs on carbonate islands that are or were tectonically active and/or have intricate interfingering of carbonate and non-carbonate rocks.

The cave and karst inventory of this study was conducted in two intensive field seasons based on information gathered during a reconnaissance survey in June 2002

(Stafford et al., 2002). During fieldwork, caves and karst features were documented, surveyed and classified by cave type. Sites of fresh-water discharge and allogenic recharge were located. Orientations of brittle failure structures were measured. After fieldwork was complete, maps were produced of the cave and karst features that were surveyed. Maps of features on Tinian were analyzed to determine cave orientation. The cave orientation data was compared to fault orientations, scarp orientations, and coastline orientations for similarity. Data comparisons were evaluated as independent data pairs both visually (rose diagrams) and statistically (Kolmogorov-Smirnov 2-sample test). Using similar techniques, Nelson (1988) and Barlow and Ogden (1992) have shown that continental, telogenetic karst development is related to the orientations of regional faults, fractures, and lineaments, implying that cave development is primarily controlled by brittle deformation.

Evaluation of the cave and karst features on Tinian and Aguijan allows them to be evaluated with the Carbonate Island Karst Model. However, the lack of previous geologic studies on Aguijan and the complex tectonic history of Tinian do not allow for simple classification of these islands.

LITERATURE REVIEW

GEOGRAPHICAL AND GEOLOGICAL SETTING

The Mariana Islands are located in the western Pacific Ocean and comprise a total of 17 islands (Figure 1). Guam is the largest and southern-most island in the Marianas and the only one that is not politically affiliated with the Commonwealth of the Northern Mariana Islands (CNMI). The relative position of the islands north of Guam in order of increasing distance is: Rota, Aguijan, Tinian, Saipan and Medinilla, which are carbonate islands. The remainder of the island chain is volcanic (Cloud et al., 1956). Tinian is located approximately 3000 kilometers east of Asia, approximately 180 kilometers north, northwest of Guam, and approximately 10 kilometers south of Saipan, while Aguijan is located approximately 9 kilometers southwest of Tinian. Tinian (Latitude: 15.01^{o}N, Longitude: 145.62^{o}E) has a surface area of 102 square kilometers with 51.2 kilometers of coastline and a maximum elevation of 187 meters (Figure 2). Aguijan (Latitude: 14.85^{o}N, Longitude: 145.57^{o}E) has a surface area of 7.2 square kilometers with 12.4 kilometers of coastline and a maximum elevation of 157 meters (Figure 3). Both islands have wet-dry tropical climates with a distinct rainy season (July-September) and dry season (February-March). Annual rainfall averages 200 centimeters and temperature ranges from 20 ^{o} to 32^{o} Celsius (Gingerich and Yeatts, 2000; Butler, 1992; Tracey et al., 1964; Doan et al., 1960; Cloud et al., 1956).

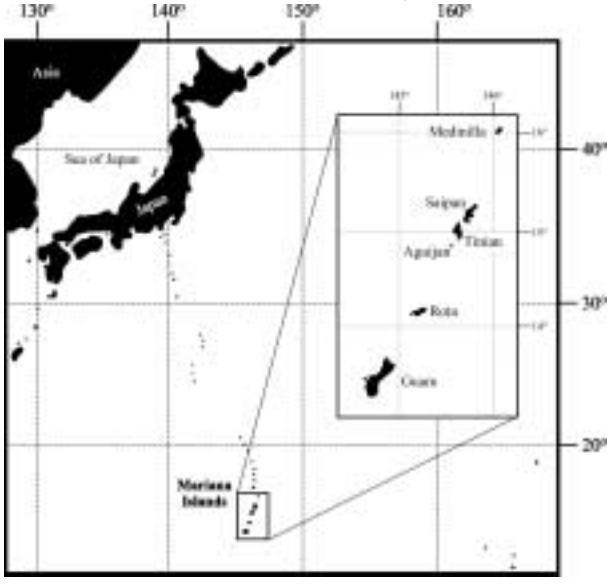

Figure 1: Location map of carbonate islands in the Marianas.

The Mariana Ridge, on which the islands of Tinian and Aguijan are located, is formed along a volcanic arc located approximately 160 kilometers west of the Mariana Trench, which is the world's deepest trench with a maximum depth of 11,035 meters (Gross, 1982). This subduction zone is created at the convergence of the Pacific Plate to the east and the Philippine Plate to the west. The Mariana Islands are situated on an older island arc that is separated by the Mariana Trough from the younger Mariana West Ridge, approximately 300 kilometers to the west, which is developing in the Mariana back-arc basin. This shift in ridge development was initiated by a change in Pacific Plate subduction geometry approximately 43 million years ago (mya) (Dickinson, 1999; Mink and Vacher, 1997; Reagan and Miejer, 1984).

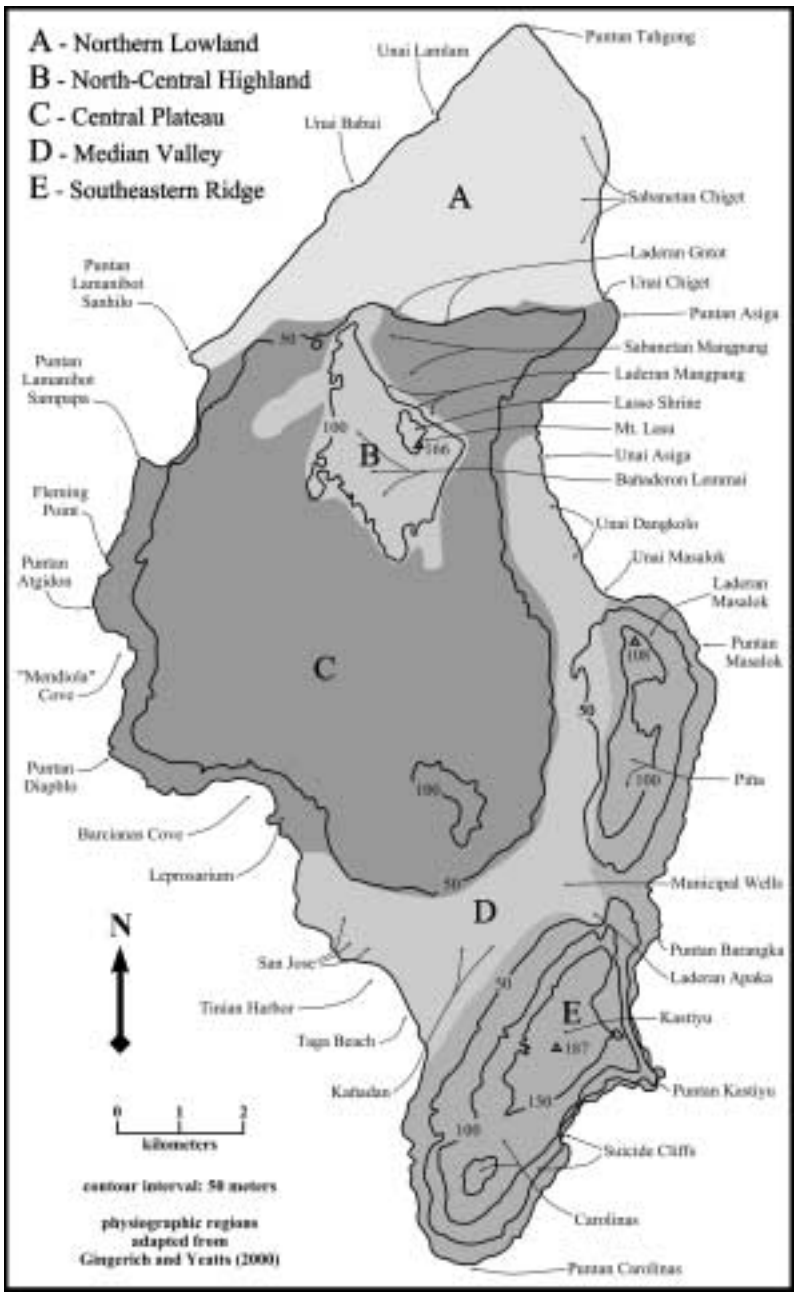

Figure 2: Physiographic map of Tinian, CNMI, with important features and locations identified (adapted from Doan et al., 1960).

Doan and coworkers (1960) used topography and spatial relationships to divide Tinian into five physiographic regions: Northern Lowland, North-Central Highland, Central Plateau, Median Valley and Southeastern Ridge (Figure 2). The Northern Lowland comprises the broad, flat, nearly horizontal surface that slopes gently upward from the west coast to Sabanettan Chiget. Located above the Central plateau and midway between the east and west coasts is the North-Central Highland, which contains the highest point (162 meters) in northern Tinian at Mount Lasu. The Central Plateau includes the central portion of the island and is isolated by steep slopes and bounding scarps associated with north-south faults. In the south and east-central regions, the Median Valley expresses little relief, but forms a broad depression bounded by faults. The Southeastern Ridge, which

includes Kastiyu, the highest point on Tinian (187 meters), is developed on two principal fault blocks (Doan et al., 1960).

Because little geologic work has been performed on Aguijan (Butler, 1992; Tayama, 1936), the following physiographic provinces are proposed based on the classification system used on Rota, which exhibits a similar terraced topography (Sugiwara, 1934): Upper Terrace, defined by elevations greater than 100 meters, which form a broad, relatively flat plateau and reaches a maximum elevation of 157 meters; Middle Terrace, defined by elevations between 50 and 100 meters, which is nearly absent on the northern side of the island and best developed on the southeastern side; and Lower Terrace, defined by elevations less than 50 meters, which includes the steep cliffs that form the coastline and the lowest bench. This classification is proposed here, in order to establish a distinction between karst development located in different regions on Aguijan (Figure 3).

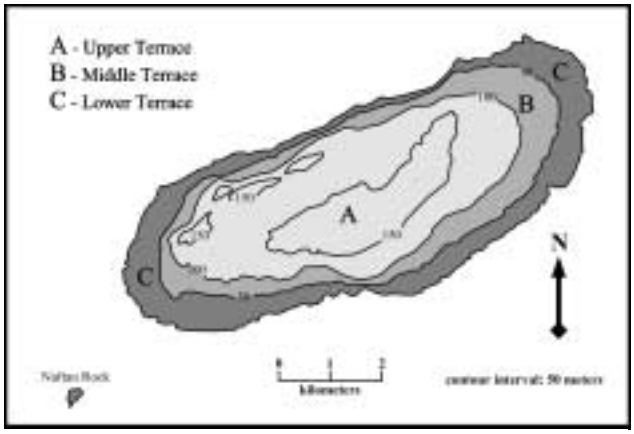

Figure 3: Physiographic map of Aguijan.

The geology of Tinian was described by Doan and coworkers (1960) and remains the most detailed geologic study for the island. Tinian is composed of volcanic tuffs and breccias covered with coralline and algal limestone (Figure 4). The igneous rocks (Tinian pyroclastic) comprise less than three square kilometers and retain only relict structures and textures because of extensive weathering. Based on the presence of foraminifera within the sediments, the

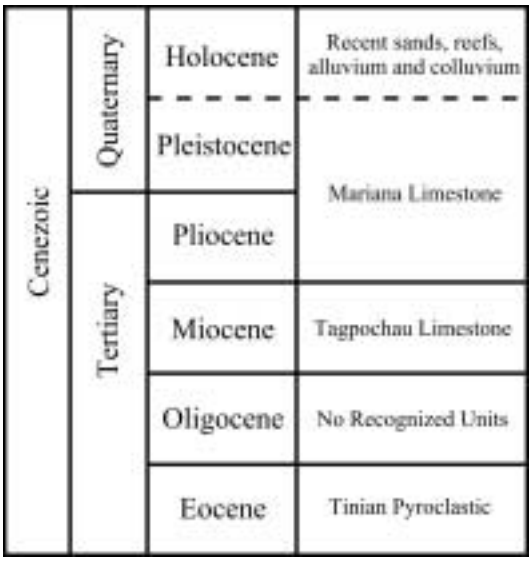

Figure 4: Geology section (adapted from Doan et al., 1960).

pyroclastics were probably ejected from a submerged vent. The limestone units are subdivided into two formations: Tagpochau Limestone and Mariana Limestone. The Tagpochau Limestone covers 16% of surface area of Tinian and is early Miocene in age. The formation is composed of three contemporaneously deposited facies: detrital (Tt), argillaceous (Tta), and sandy (Tts). The detrital facies comprises the majority of the formation and is composed primarily of fragments of biogenic calcium carbonate with calcite cement. The other two facies comprise only a small portion of the Tagpochau Limestone. The Mariana Limestone covers 83% of the surface area of Tinian and was deposited in Pliocene and Pleistocene time. The formation was subdivided based upon the presence of constructional or detrital compositions into seven facies: constructional coralliferous facies (Qtmcc), constructional algal facies (QTmca), detrital coralliferous facies (QTmc), detrital shelly facies (QTms), detrital *Halimeda* facies (QTmh), detrital argillaceous facies (QTmu), and detrital undifferentiated facies (QTmu). Overlying these deposits in coastal regions are Holocene limestones, developing sands and gravels, and reefs (Siegrest, 1988; Doan

et al., 1960; Burke, 1953). Recent fieldwork indicates that late Pleistocene limestones may also overlie the Mariana Limestone, because some limestone present in coastal areas appears to correspond with oxygen isotope stage 5e, suggesting that Mariana Limestone deposition does not extend to the Pleistocene/Holocene boundary (Stafford et al., 2002).

While no detailed study of the geology of Aguijan has been conducted, the same classification for rock units used on Tinian will be applied, based on its close proximity, until future work produces a more detailed geologic map of Aguijan. In addition, it is presumed that Aguijan is similar to other islands in the southern Marianas, in that a non-carbonate core of pyroclastic rocks exists beneath the exposed carbonate rocks that crop out, while the development of three distinct terrace levels on Aguijan suggests a similar tectonic history (Stafford et al., in press; Doan et al., 1960; Sugiwara, 1934).

HISTORICAL SETTING

The Mariana Islands were first settled by the Chamorro people around 1500 B.C.E. (before common error). In 1521, Ferdinand Magellan, discovered the Marianas and named them *Islas de los Ladrones* (Islands of the Thieves), which were then renamed *Islas de las Marianas* (Islands of the Marianas) in the early 1600's after Maria Ana of Austria, the widow of the Spain's king, Phillip the IV. The islands remained in Spanish control for almost four centuries, during which time much migration by indigenous people from the Caroline Islands occurred. In 1899, after Spain's loss of the Spanish-American war, the Spanish controlled islands of Micronesia (Mariana Islands, Caroline Islands and Palau) where sold to Germany. During German control, the northern Marianas greatly developed agricultural and fishing economies by immigrating additional Carolinian people from Chuuk and Yap, as well as Japanese people from nearby islands like Okinawa, who developed a lucrative agricultural trade market of copra and sugar cane. German control lasted until World War One (Hunt and Wheeler, 2000).

In 1914 Japan took control of the Mariana Islands at the start of World War One. After the war, Japan's control as administrator was recognized by the League of Nations and remained so until World War Two. During the Japanese occupation, vast tracts of land were cleared of coconut trees and tropical forest, so that the extensive sugar cane plantations could be developed covering 58% (Bormann, 1992) to 90% (McClure, 1977) of the land area. In 1944, United States military forces secured the islands in some of the bloodiest battles of World War Two. Tinian became instrumental in America's Pacific war campaign. The northern third of the island was developed into a large airbase named North Field, consisting of four major runways. During full operation, this was the largest and busiest airfield in the world with two B-29's taking off simultaneously every 45 seconds on mission days. From North Field, the two atomic bombs, Fat Man and Little Boy, were assembled and loaded into the B-29 bombers Enola Gay and Bock's Car for drops on Hiroshima and Nagasaki, respectively (McClure, 1977).

In 1947, the United Nations gave the United States trusteeship over the Mariana Islands, which continued until the 1970's. In 1970 discussion began between the Marianas and the United States over the termination of the trustee agreement, which led to a plebiscite in 1975, which negotiated a covenant with the Unites States. The *Covenant to Establish a Commonwealth of the Northern Marianas Islands in Political Union with the United States of America* negotiated an agreement where the citizens of the Northern Mariana Islands became self-governing as a Commonwealth, while Guam remained a United States territory. The covenant enabled the Commonwealth of the Northern Mariana Islands (CNMI) to retain the benefits of U.S. citizenship, excluding the right to vote in U.S. presidential elections, which ensured continued economic support. In exchange,

the U.S. was given lease of 75 square kilometers of land in the Northern Mariana Islands, including over two thirds of Tinian (Hunt and Wheeler, 2000).

Today, Tinian and Aguijan are governed by a single municipality as part of the Commonwealth of the Northern Mariana Islands (CNMI). Aguijan is uninhabited and Tinian hosts a population of approximately 2000 individuals. While the majority of the Tinian remains under U.S. military control, small farms and tourism, including scuba diving and casinos, provide commerce (Bormann, 1992).

CARBONATE ISLAND KARST

This study enables the studies in karst geology and hydrology performed on Guam (Mylroie et al., 2001) and in the Caribbean and Atlantic (Frank et al., 1998; Mylroie and Carew, 1995a; Mylroie et al., 1995a) to be applied and evaluated to different settings. A primary objective of investigation on Tinian is to advance the understanding of the karst hydrology of carbonate islands, while refining the general Carbonate Island Karst Model (CIKM). The Carbonate Island Karst Model has been designed as the definitive model for the hydrologic development of island karst. Modern carbonate islands are unique due to extensive interaction between fresh and saline groundwater within young, porous rock, which produces a unique geologic and hydrologic history that is different than that in continental settings (Vacher and Mylroie, 2002; Mylroie and Jenson, 2002; Mylroie et al., 2001; Mylroie and Vacher, 1999, and references therein).

Karst forming in marine conditions on carbonate coasts and islands can be explained by the Carbonate Island Karst Model (Figure 5) (Stafford et al., 2003; Jenson et al., 2002; Mylroie and Jenson, 2002; Mylroie and Jenson, 2001). Its main aspects are:

1. The fresh water/salt water boundary creates mixing dissolution, and produces organic-trapping horizons at both the upper and lower boundaries of the fresh-water lens.
2. Glacio-eustacy has moved the fresh-water lens up and down through a vertical range of over 100 m in the Quaternary.
3. Local tectonics can overprint the glacio-eustatic sea level events, adding complexity to the record.
4. Carbonate islands can be divided into four categories based on basement/sea level relationships:
   i. Simple carbonate islands (no non-carbonate rocks).
   ii. Carbonate cover islands (non-carbonate rocks beneath a carbonate veneer).
   iii. Composite islands (carbonate and non-carbonate rocks exposed on the surface).
   iv. Complex islands (faulting and facies interfingering create complex carbonate/non-carbonate relationships).
5. The karst is eogenetic, *i.e.*, it has developed in carbonate rocks that are young and have never been buried below the range of meteoric diagenesis.

Carbonate islands described by the Carbonate Island Karst Model are composed of young limestones and are heavily influenced by meteoric waters and mixing-zone dissolution, creating an environment for eogenetic karst to develop because of their close proximity to the site of deposition. Vacher and Mylroie (2002, p. 183) define eogenetic karst as "the land surface evolving on, and the pore system developing in, rocks undergoing eogenetic, meteoric diagenesis." Eogenetic carbonate rocks are diagenetically young and have not undergone extensive cementation and compaction, as opposed to telogenetic carbonate rocks that are diagenetically mature, have been buried below the range of meteoric diagenesis, and are currently

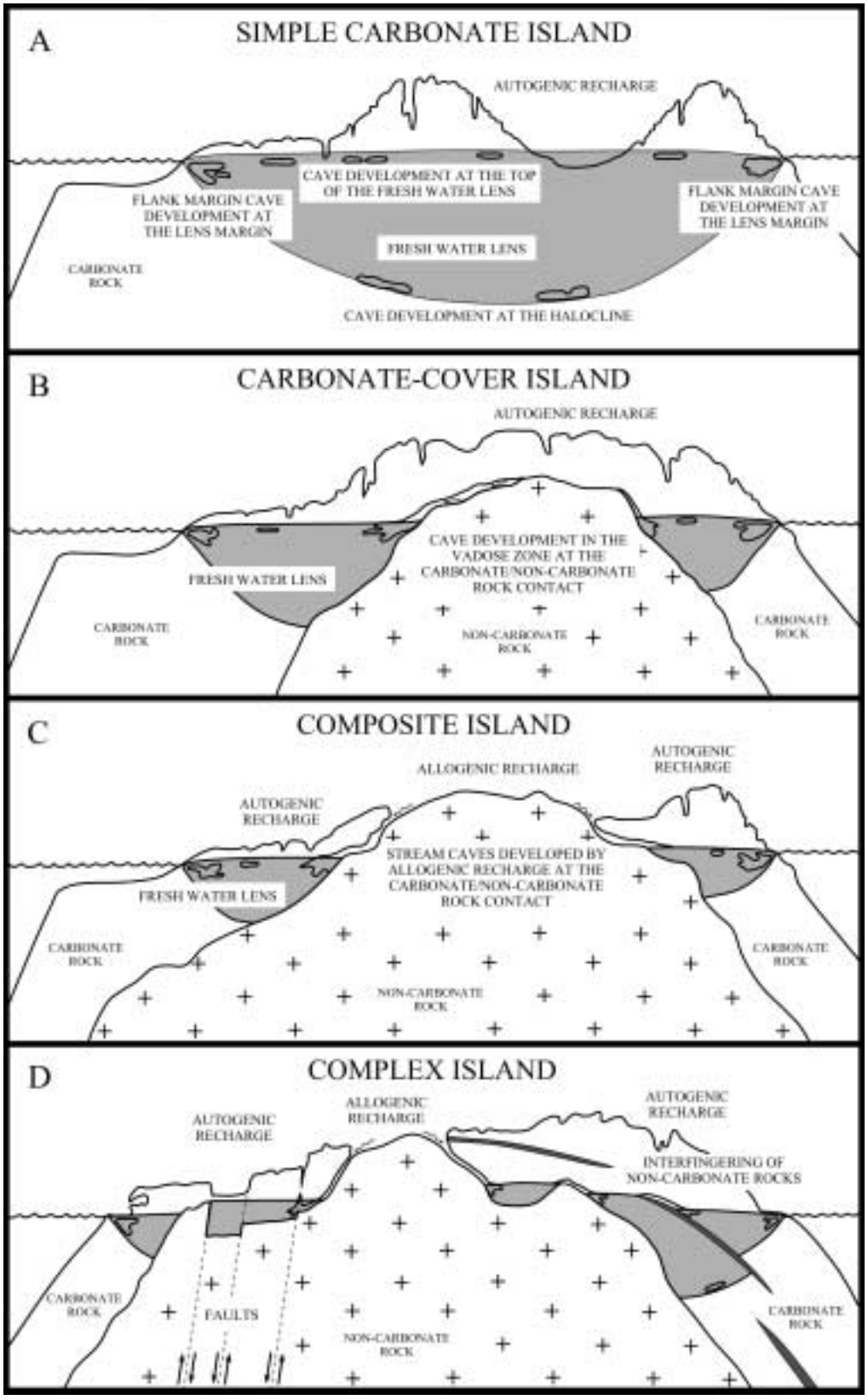

Figure 5: Carbonate Island Karst Model (CIKM) (adapted from Mylroie et al., 2001).

exposed at the earth surface by tectonic uplift and erosion of overlying strata (Klimchouk and Ford, 2000). Typically, small carbonate islands are the sites of eogenetic karst undergoing meteoric diagenesis, however, it is not possible to state that carbonate islands develop solely eogenetic karst and continental settings develop solely telogenetic karst, because fresh-water / sea-water interaction and a fresh-water lens affected by glacio-eustacy are also required for the formation of carbonate island karst, as defined by the Carbonate Island Karst Model (Jenson et al., 2002; Mylroie and Jenson, 2002).

Eogenetic karst development occurs on islands such as Bermuda, the Bahamas, and the Marianas, as well as in continental settings such as the Biscayne aquifer of Florida, where the carbonate rocks are young. Telogenetic karst development occurs on islands such as Gotland (Sweden) and Kephallenia (Greece), as well as in continental settings such as Kentucky (United States) and England (Great Britain), where the rocks are of appreciable age and have been buried beyond the range of meteoric diagenesis (Vacher and Mylroie, 2002). Because eogenetic karst and island karst are not necessarily synonymous, a distinction should be made between *island karst* and *karst on islands*. *Island karst* occurs in specific environments that must include three basic parameters: 1) interaction of fresh-water and sea-water, which produces mixing zone dissolution, 2) a fresh-water lens that was affected by glacioeustatic changes in the Quaternary, and 3) karst that is eogenetic. *Karst on islands* may exhibit some of the characteristics of *island karst*, but these islands are not true *island karst* unless all three basic parameters are present. Islands like Jamaica and Puerto Rico have karst landforms (e.g. cockpits and mogotes) in their interior that are developed in rocks of appreciable age and that are not influenced by glacio-eustacy or fresh-water / salt-water interaction. This makes the karst landforms *karst on islands*. True *island karst* occurs on islands like the Bahamas, where the rock is diagenetically young, fresh-water interacts extensively with the salt-water, and the fresh-water lens has been significantly affected by glacio-eustacy. Therefore, islands that have telogenetic karst, are removed from the affects of glacio-eustacy, and/or do not exhibit mixing zone dissolution should have karst landforms and features reported as *karst on islands*, while islands that exhibit eogenetic karst, are affected by glacio-eustacy, and exhibit mixing zone dissolution should have karst landforms and features reported as *island karst* (Vacher and Mylroie, 2002).

In eogenetic rocks that have not undergone compaction and cementation, the rocks tend to initially exhibit high matrix porosity and moderate permeability, but can develop secondary vuggy porosity as a result of meteoric and fresh-water diagenesis. The matrix porosity will generally decrease with age as secondary cementation infills the pore space, while permeability increases as preferential flow develops extensive horizontal flow routes. Over time, the bulk porosity remains the same or decreases, but the vertical hydraulic conductivity of the rock decreases while the horizontal hydraulic conductivity increases (Vacher and Mylroie, 2002). Due to the proximity of eogenetic karst to marine waters in island settings, it is highly susceptible to changes in sea level, which results in the migration of the fresh-water lens and flow routes in response to glacioeustatic and tectonic changes.

The four conceptual model classifications of carbonate islands are based on island composition (Figure 5). *Simple carbonate islands* are composed of only carbonate rocks at the surface and to a depth below the base of the fresh-water lens (Figure 5A). The Bahama Islands are a good example. *Carbonate cover islands* are composed of only carbonate rocks at the surface, but have non-carbonate rocks that interact with the fresh-water lens without being exposed at the surface (Figure 5B). Bermuda is a good example. Carbonate

cover and simple carbonate islands can easily shift from one form to the other as a result of changes in relative sea level (Figure 6). *Composite islands* are composed of both non-carbonate and carbonate rocks on the surface (Figure 5C). Barbados is a good example. These three island types represent a classification scheme where the two end member environments are islands completely composed of carbonate rocks at one end and islands completely devoid of carbonate rocks at the other end, with intermediate compositions described by the model (Figure 6). The fourth type are *complex islands*, which are characterized as having complex geologies as a result of faulting, the interfingering of different lithologies, and the presence of both carbonate and non-carbonate rocks (Figure 5D). Guam and Saipan are excellent examples (Jenson et al., 2002; Mylroie et al., 2001).

In traditional continental settings, structural and lithologic controls have been recognized as having a significant influence on karst development. Klimchouk and Ford (2000, p. 57) state: "Bedding planes, joints, and faults are planar breaks that serve as the principal structural guides for groundwater flow in almost all karstified rocks." In island karst settings the significance of structural and lithologic controls have often been overlooked because of the dominant role of mixing-zone dissolution in the hydrogeologic system and because the original models for island karst were developed on simple carbonate islands in the Bahamas. Jenson and coworkers (2002) and Mylroie and coworkers (2001) have recently recognized the importance of structural and lithologic controls on carbonate island karst by modifying the CIKM with the addition of the fourth type, the complex island. This addition enables the effects of deformation

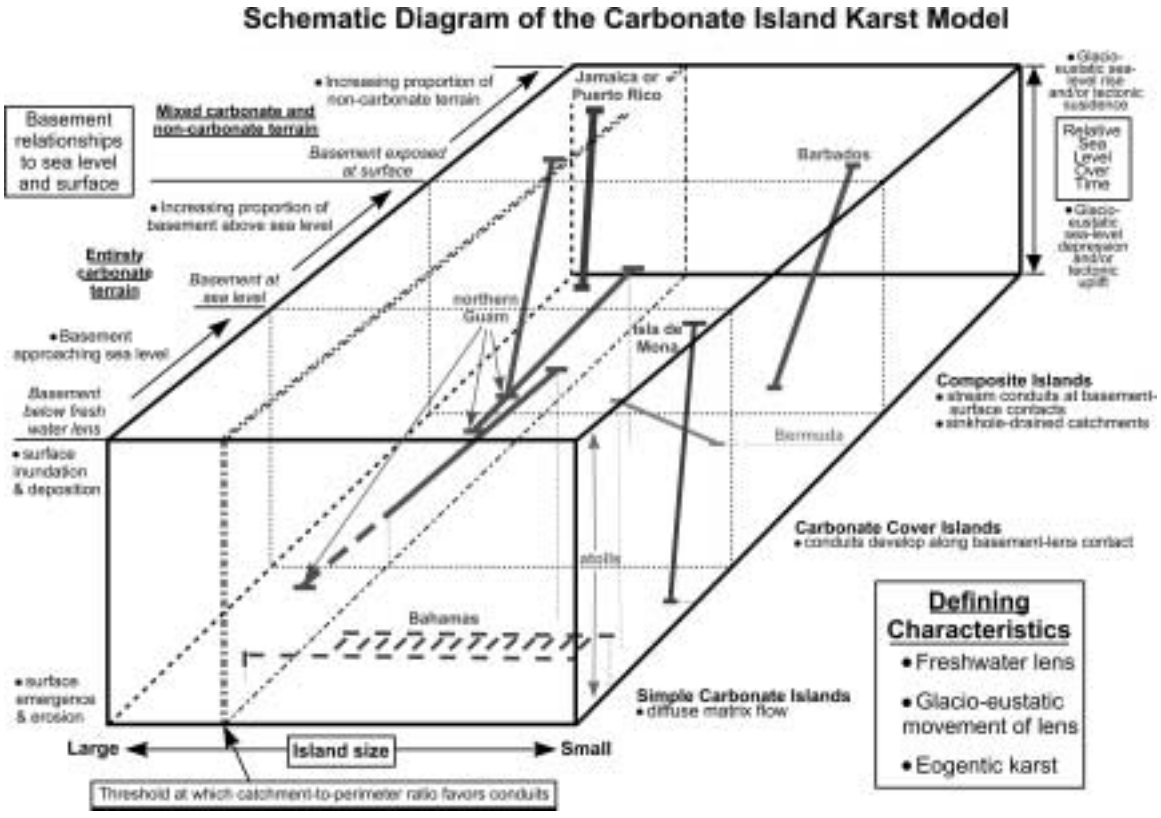

Figure 6: Schematic diagram illustrating the relationship between island size, basement relationships to sea level and surface, and relative sea level for simple, carbonate-cover, and composite islands within the Carbonate Island Karst Model (CIKM) (Mylroie and Jenson, 2001, Fig.2, p. 54).

and lithology to be accounted for on carbonate islands that are or were tectonically active and/or have intricate interfingering of carbonate and non-carbonate rocks.

Lithologic controls include variations in rock composition between rock formations and within the same rock formation, where beds subdivide the unit. Variations may include grain size, grain origin, grain sorting, and chemical composition. These variations provide routes for preferential dissolution within beds and formations of favorable composition, while less favorable beds and formations may restrict dissolution and fluid movement (Klimchouk and Ford, 2000; Sasowsky and White, 1994; Palmer, 1991; White, 1988).

Structural controls include both brittle and ductile deformation. Ductile deformation results in the folding of rock bodies, which adds to the complexity of lithologic controls. Brittle deformation includes joints, fractures, and faults, which are often found in tectonically active, carbonate islands where uplift and subsidence create complex geology. Fractures are surfaces where the rock has been broken, occur over a range of centimeters to meters and fall into several categories, including: extension – relative rock motion is perpendicular to the surface; shear – relative motion is parallel to the surface; and oblique – relative motion is a both parallel and perpendicular to the surface. Joints are specific types of fractures, which show only minor extension (Twiss and Moores, 1992). Fractures reported on Tinian and Aguijan are primarily associated with gravity slides resulting from bank margin or cliff margin failure along steep scarps. Joints reported occur inland of the bank margin/cliff margin fractures, possibly as a result of rock expansion from a decrease in lateral pressure from the scarp failure or as unloading structures associated with isostatic subsidence, and perpendicular to coastlines, which may be associated with coastal erosion or regional faulting (Stafford et al., 2002). Faults are surfaces or narrow zones that show relative displacement similar to fractures, but over larger regions and generally associated with regional tectonics (Twiss and Moores, 1992). Faulting is reported throughout Tinian, including the boundaries between the Southeastern Ridge and the Median Valley and between the Central Plateau and the Northern Lowland, where fault blocks moved independently during island emergence (Doan et al., 1960).

Joints, fractures, and faults generally enhance fluid movement, but may also restrict it. Enhanced flow can occur along planar features that provide a surface for fluid movement both laterally and vertically across lithologic boundaries, creating greater connectivity within the subsurface. Restricted flow can result if recrystallization (slickensides) or secondary infilling (caliche dikes) develop along the planar surface, creating a barrier for fluid movement. Flow restriction may also occur if faulting results in the offsetting of different rock units, which produces contacts between carbonate and non-carbonate rocks that did not previously exist (Klimchouk and Ford, 2000; Sasowsky and White, 1994; Palmer, 1991; White, 1988).

KARST FEATURES

Karst features on Tinian can be classified into four broad categories; epikarst, closed depressions, caves, and discharge features. Identification, classification, and spatial distribution of different karst morphologies provide a basis for understanding the hydrology of the region.

Epikarst

Epikarst is the zone of dissolutional sculpturing (karren) that is present on the surface and upper few meters of bedrock in carbonate regions. Karren has been described as minor solutional forms, which range from millimeters to meters in scale (White, 1988). In general, epikarst is independent of environmental setting; however, in coastal regions, where salt spray

is in active contact with carbonate rocks, an environment is created for the production of biokarst (Viles, 1988) or phytokarst (Folk et al., 1973); however, the biological affects are often overstated (Mylroie and Carew, 1995b). The surface of the karren in eogenetic karst is generally extremely rough and may not support extensive soil profiles because soil-forming material is in short supply. Taborosi and coworkers (in press) have recently reported additional karren morphologies on eogenetic karst on Guam. In the Mariana Limestone on Guam most weathered surfaces are extremely jagged and reminiscent of biokarst or phytokarst and is attributed to a polygenetic origin that includes mixing dissolution from rainwater mixed with salt spray, salt weathering, dissolution by meteoric waters, and biological weathering (Taborosi et al., in press). However, other karren morphologies are also present, which include more rounded karren in inland regions and dissolution along brittle failure planes producing enlarged vertical and horizontal joints as wells as solution pans (kaminetzas) (Taborosi et al., in press). Carbonate rocks on most islands generally have little insoluble material to produce soils, suggesting that the insoluble material is exclusively of eolian origin. The soils that are present are generally piped downward into voids and dissolutional cavities within the karst system. Eogenetic karst regions have specific vegetation types because of the limited development of soils, which affects infiltration rates of water entering the karst system based on soil thickness, composition and its presence, absence or modification (human development). Beneath karren, dissolutional bedrock debris, and soil, which comprise the surficial epikarst, the remainder of the epikarst zone is composed of solutional fissures, holes, and shallow small cavities in the bedrock (Mylroie et al., 2001). Epikarst contributes water to the deep vadose zone as diffuse flow and through the integration of flow paths created by cavities and fissures in the lower epikarst. This integrated flow can effectively bypass the deep vadose zone via fractures and pits and supply water directly to the phreatic zone (Mylroie et al., 1999). Epikarst development and extent is a primary controlling factor on the quantity of water that enters phreatic storage via vadose paths and it is possible that it may serve as a location of significant water storage (Jocson et al., 2002; Jocson et al., 1999; and Jenson et al., 1997). Epikarst on Tinian appears identical to that seen on Guam and Saipan (Taborosi, 2000).

Individuals involved in the development of land in karst regions dominated by epikarst should be aware that any modifications to the land surface and epikarst would alter the drainage dynamics of the area. Ponding basins may actually exhibit lower infiltration rates because of high sediment loads. Runoff events and soil erosion may also increase as a result of the modification of the natural landscape (Mylroie and Carew, 1997).

Closed Depressions

In carbonate island environments, closed depressions can be classified into three general categories: dissolution, natural construction, and human modification. These different types can be extremely hard to differentiate based on appearance and it is possible that the features may have been any or all of the three classification types at some point in their development. In carbonate islands, dissolutional depressions are generally small to moderate in size as a result of their young age and the nature of autogenic recharge. However, in areas where non-carbonate rocks are exposed at the surface, streams can develop that provide allogenic recharge to the karst system, possibly forming large depressions as are seen on Guam (Mylroie et al., 2001; Taborosi, 2000). Natural construction depressions are those that formed at the time the rocks were deposited or are the result of subsequent deformational processes. Mylroie and coworkers (2001) report that natural construction depressions are the most common form on simple carbonate

islands, and anthropogenic depressions (e.g. quarries, landfills, artificial drainage ponds, and storage ponds) are often constructed in these pre-existing features (Mylroie et al., 1999).

Tinian exhibits areas where dissolution-type closed depressions are formed. Dissolution depressions have been seen at the contacts between exposed volcanic outcrops and carbonate outcrops (Stafford et al., 2002). On Tinian, four exposures of volcanic rocks are recorded near Sabanettan Mangpang, Bañaderon Lemmai, and Laderan Apaka. At the three northern locations (two at Sabanettan Mangpang and one at Bañaderon Lemmai), there are closed depressions in the limestone outcrops, which show allogenic streams descending into them from the volcanic outcrops. An initial field investigation of Bañaderon Lemmai has shown that these features are similar to those seen on Guam and are providing point source recharge into the karst system (Stafford et al., 2002). In the south-central region near Laderan Apaka, volcanic outcrops are exposed on a north-facing cliff. To the north of the outcrops, a large closed depression (Sisonyan Makpo) exists in which the Municipal Wells are located (United States Department of the Interior Geological Survey, 1983), which may be a natural construction feature formed by complex faulting on the island, based on its location between the two prominent ridges (Kastiyu/Carolinas and Piña) of the Southeastern Ridge and the low-lying Median Valley. Weathering of volcanic rocks and talus accumulation may be partially armoring the slopes of the cliff and the closed depression, increasing recharge to the closed depression and possibly leading to lateral corrosion of the closed depression.

Throughout Tinian, human-modified depressions are also commonly reported (United States Department of the Interior Geological Survey, 1983) and may represent modified constructional depressions similar to those reported on other carbonate islands (Mylroie et al., 1999). These include modern and ancient quarries (latte stone), borrow pits, refuse disposal sites, artificial drainage ponds in residential areas, and features associated with World War Two (bomb pits, defensive positions, etc.). Initial field investigations have revealed that significant natural depressions are found in association with volcanic outcrop exposures. The large closed depressions seen elsewhere are probably natural construction features or features produced by human modification, possibly to pre-existing natural depressions, of the land surface (Stafford et al., 2002).

Caves

Caves are natural openings in the earth that can be characterized based on their size, shape, length and overall geometry (White, 1988). Solution caves, which have been formed by the dissolution of bedrock by circulating groundwater, are present throughout the islands of Tinian and Aguijan. Solution caves on carbonate islands can be grouped into various categories. In the Mariana Islands, five distinct cave types have been documented: banana hole, flank margin cave, fissure cave, pit cave, and stream cave (Figure 7). In some areas, it is difficult to discern the exact origin and original extent of some caves, because of the extensive modification of some features for Japanese military purposes during World War Two (Taborosi and Jenson, 2002). In addition to human modification, horizontal notches cut into cliff faces create an additional classification problem. Traditionally these have been identified as bioerosion notches, but may also form by lateral corrosion and cliff retreat, or they may be the remnants of flank margin caves (Mylroie et al., 1999). Accurate classification of karst features is integral to interpreting the hydrogeology of island karst.

Banana holes (Figure 7) are shallow, small chambers that formed at the top of the fresh-water lens. They are isolated features and exhibit a morphology with a width to depth ratio greater than one (Harris et al., 1995). On Tinian no feature has been currently identified as a definite banana

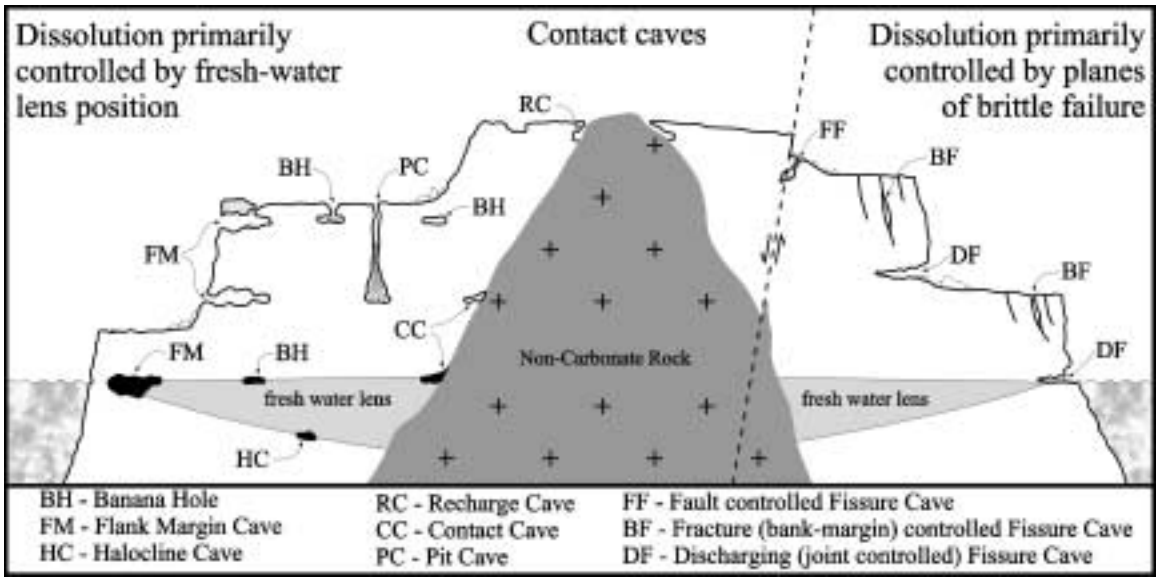

Figure 7: Conceptual model of cave types that form in eogenetic rocks on carbonate islands.

hole. A feature located several hundred meters to the northwest of the Lasso Shrine appears to have a complex history that could be explained as the stacking of two or more banana hole features vertically on one another as sea level fluctuated. Later collapse by upward stoping could then form the collapsed areas seen in the lower levels of this feature (Stafford et al., 2002).

Flank margin caves (Figure 7) are formed in the distal margin of the freshwater lens where thinning of the lens and mixing of fresh and saline waters creates dissolutionally aggressive phreatic waters (Mylroie et al., 1995a) and are the most common morphology type that has been reported on Tinian (Stafford et al., 2003, 2002). Flank margin caves exhibit globular morphologies with a wide range of sizes that may be connected, but often remain as isolated chambers. Flank margin caves can be used as indicators of previous sea-level stillstands and have potential as tools for evaluating differential rates of uplift in tectonically active carbonate islands (Carew and Mylroie, 1995; Mylroie et al., 1995a,b). Flank margin caves may collapse in coastal regions to form coves and caletas, which retain only remnants of the original cave morphology (Back et al., 1984). Further complicating the morphology and identification of flank margin caves are bioerosion notches formed by wave erosion and invertebrate borings at sea level during stillstands (Mylroie and Carew, 1991).

Flank margin caves have been reported at various locations. The most significant flank margin cave development is in the Suicide Cliffs on the southern end of Tinian, were numerous entrances can be seen inland from the road on the southern coastal terrace. These caves are located approximately 50 meters upslope from the lower terrace and are developed along a consistent horizon that is believed to reflect a past sea-level stillstand. Along the northern edge of the Southeastern Ridge, near Laderan Apaka, a series of flank margin caves are located, which are less extensive due to more complete erosion and slope retreat. Near Lasso Shrine on northern Tinian, a series of modified flank margin caves are located in the eastern cliffs. Along the east coast, flank margin caves that are at various stages of erosion due to cliff retreat and coastal erosion are present near Unai Masalok and Unai Dangkolo. At Unai Dangkolo, the largest flank margin cave documented on Tinian is located approximately 200 meters inland. This cave

is breached on the surface by ceiling collapse and can only be entered from above via a 10-meter descent. The cave consists of several large chambers that intersect, creating a complex system that is laterally extensive covering and area greater than 1300 square meters with cave passages developed around a central chamber approximately 15 meters tall and 35 meters in diameter (Stafford et al., 2002).

Fissure caves (Figure 7) are developed along joints, fractures, or faults, in which preferential flow along the planar surface has resulted in enhanced dissolution rates (White, 1988). Three basic types of fissure caves have been identified, based on their morphology and spatial relationship to the island. At the coastal edge, development perpendicular to the coastline has been reported, which in several cases has resulted in caves that often discharge freshwater and penetrate inland up to 30 meters as tubular passages with distinct joints located in their ceilings. The second type has formed as fractures parallel to the coastline or scarps as a result of cliff-margin or bank-margin failure. These fractures may reach the water table where they can affect the flow dynamics of the lens by locally distorting the lens or by providing vadose routes that intercept the normal diffuse flow in the phreatic zone (Mylroie et al., 1995c; Aby, 1994). Dissolutionally enhanced fractures have produced caves over 40 meters deep on Tinian. The third type occur where dissolution along a fault plane, in conjunction with collapse, has formed caves, which tend to develop at moderate to steep angles along the dip of the fault, and the caves extend laterally along the strike of the fault. All three types of fissure caves are hydrologically important because they provide vadose fast flow routes for water through the subsurface, either as recharge or discharge features and may distort the local lens morphology and flow dynamics (Stafford et al., in press; Stafford et al., 2002).

Pit caves (Figure 7) are vertical shafts that have developed by the dissolution of descending meteoric waters and have a depth to width ratio greater than one. Pit caves often develop as a series of shafts with connecting lateral sections, act as vadose fast-flow routes for water entering the subsurface, and effectively drain the epikarst (Mylroie and Carew, 1995a). Although common in certain settings (Harris et al., 1995; Mylroie and Carew, 1995a), only one pit cave has been reported on Tinian. It is located 10 meters from the cliff edge on the south coast, where it connects to a low-level bench just above sea level. It is approximately 25 meters deep with an entrance width of 3 meters, but due to its location and near-direct connection to the ocean, it has little effect on aquifer recharge. However, its presence indicates the possibility of other similar features in the area, which may be covered at the surface by collapse and at shallow depths could be open, acting as vadose fast flow routes (Stafford et al., 2002).

Stream caves (recharge caves, Figure 7), hydrologically active caves that are fed by allogenic water, have been documented in regions were contacts between carbonate and non-carbonate rocks occur. Meteoric water is unable to infiltrate efficiently into the volcanic rocks, and forms surface streams, which channel water to the outcrop periphery where it descends into the carbonate rocks as point source allogenic recharge (Mylroie et al., 2001).

Tinian volcanic rocks outcrop in four regions and closed depressions are associated with the periphery of each of these outcrops. Due to time and logistics, only one of these features, located to the east of the largest outcrop at Bañaderon Lemmai, was investigated in June 2002 (Stafford et al., 2002). This site contains a large sinkhole that appears to be armored with volcanic sediments that restrict infiltration, but on the eastern edge, a small cave is present that shows evidence of allogenic recharge during rain events (Stafford et al., 2002). It is expected that other closed depressions associated with these volcanic outcrops will exhibit similar features formed

by dissolution at the non-carbonate/carbonate contact, with variations dependant on sediment infilling and the volume of allogenic recharge that is received.

Discharge Features

Discharge volume and types vary greatly on carbonate islands and spatially within the same island. Three general categories of discharge features can be defined: seeps, springs, and submarine freshwater vents. Of these types, seeps represent diffuse discharge, while the other types represent focused discharge points. Seeps occur extensively in coastal areas where calcareous sand covers the bedrock and disperses emerging water over a large area. Springs are locations in which water emerges from the bedrock along preferential flow paths generally defined by bedding planes or fractures along coastlines. Springs may be laterally extensive if controlled by bedding planes or they may be restricted to a single point discharge if controlled by fractures. Submarine freshwater vents are areas where freshwater discharge occurs below tidal level along the island periphery (Jocson et al., 2002; Mylroie et al., 1999).

Seeps and springs have been documented in coastal regions on Tinian. Minor seeps are present at Unai Dangkolo and Unai Masalok on Tinian, while springs have been documented in various coastal areas. On Tinian, fracture caves were reported along the west coast near Unai Masalok where freshwater could be observed mixing with salt water and discharging from solutionally widened bedding planes that extend approximately 30 meters inland (Stafford et al, 2002). Submarine freshwater vents are not reported for Tinian and Aguijan, but features are expected to exist that are similar to those that have been reported from Guam (Mylroie et al., 2001; Jenson et al., 1997), where freshwater discharges below sea level.

WATER RESOURCES

Fresh-water is partitioned in a lens above salt-water and is affected by the presence of non-carbonate rocks interacting with the fresh-water lens. Basal water occurs where the fresh-water lens is directly underlain by sea-water, while parabasal water occurs where the fresh-water lens is directly underlain by non-carbonate, basement rocks (Figure 8; Mink and Vacher, 1997). Basal waters develop a lens thickness defined by the Ghyben-Herzberg Principle:

$$Z = [(\rho_f)/(\rho_s - \rho_f)]h,$$

where Z is the depth of the fresh-water lens below sea level, h is the height of the lens above sea level, and ρ_f and ρ_s are the densities of fresh-water and salt-water respectively (Figure 8; White, 1988; Raeisi and Mylroie, 1995). The fresh-water/salt-water lens thickens as the fresh-water head depresses the interface below sea level, relative to the density difference in the two waters:

$$Z = \alpha h,$$

where $\alpha = (\rho_f)/(\rho_s - \rho_f)$. With ρ_f = 1:00 g/cm^3 and ρ_s = 1.025 g/cm^3, $\alpha = 40$; therefore, for every one meter or foot of fresh-water head, the fresh-water/salt-water interface is depressed 40 meters or feet (1:40 ratio) (White, 1988; Raeisi and Mylroie, 1995).

Island environments have limited water resources and specific problems because of the morphology of the fresh-water lens (water with a chloride concentration <250 mg/L (Gingerich and Yeatts, 2000)). Because of the limited extent of island aquifers and the characteristics of eogenetic karst, island aquifers are extremely susceptible to contamination. Contamination from the surface can include: human and animal wastes, fertilizers, detergents, pesticides, herbicides, petroleum spills, and solvent spills. Subsurface contamination can occur from salt-water

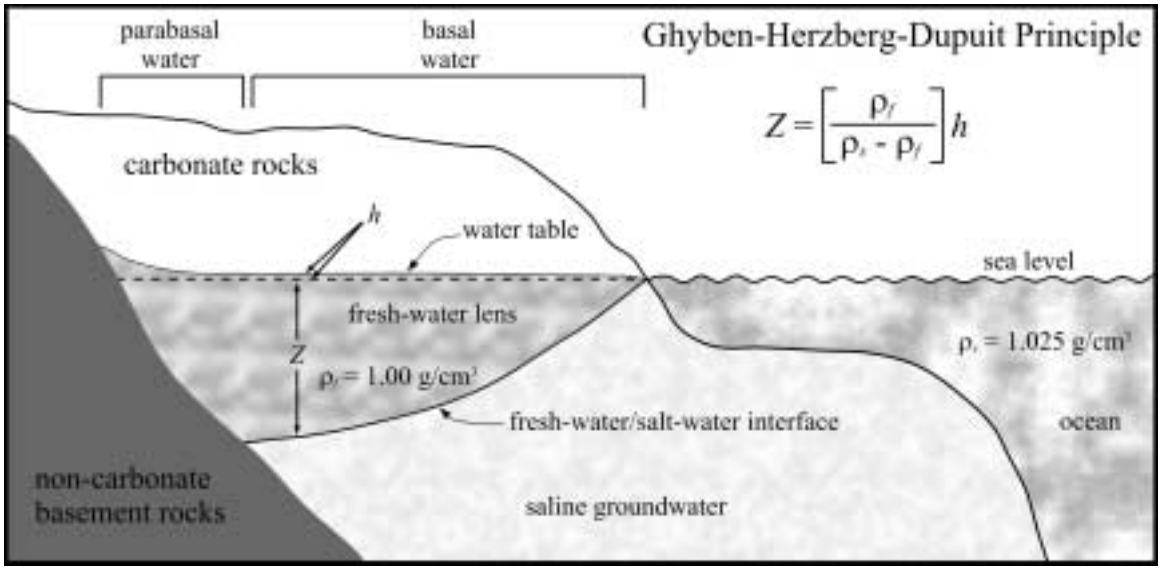

Figure 8: Model showing the fresh-water lens morphology showing the location of basal and parabasal waters and the Ghyben-Herzberg principle (adapted from Mink and Vacher, 1997 and Raeisi and Mylroie, 1995).

intrusion, where over pumping produces a cone-of-depression in the lens, which then up-cones salt-water into the fresh-water lens at a one to forty ratio. Because of the ratio of up-coned water to lens thickness above sea level, a small decrease in the lens thickness above sea level will create a large cone of depression at depth in basal waters (Gingerich and Yeatts, 2000; Mylroie and Carew, 1997). When non-carbonate rocks extend into or through the freshwater lens, basement rocks restrict upconing of parabasal water because salt-water does not directly underlie fresh-water. Therefore, it is important for island communities to effectively manage their water resources in order to continue to produce potable water, by limiting water extraction at specific sites and by utilizing zones of parabasal groundwater (Mink and Vacher, 1997).

In the 1995 census, 2,631 people were listed as living on Tinian primarily in the Median Valley and parts of the adjacent Central Plateau, which comprises 25% of the total island surface area. This limited region of population is partially the result of the United States control of the northern third of the island, the Northern Lowland, for military purposes, while other regions are less accessible due to terrain. Of the inhabited region, 60% is an undeveloped, public, rural area. The remaining 40% of this region is composed of residential and commercial lots that include a casino resort, small businesses, farming, grazing and housing. The residential and commercial lots provide the largest concerns for contamination from surface spills and biological waste disposal. Tinian currently has no sewer facility, instead human waste is disposed of through septic and seepage tanks, leaching fields or holding tanks, which may not be adequate for preventing groundwater contamination, because of the thin soil profile and rapid infiltration rates associated with eogenetic, carbonate rocks. Other sources of contamination include the airport, several quarries and a solid waste disposal dump, which provide paths for direct recharge into the aquifer by bypassing the soil surface and epikarst, which have been removed (Gingerich and Yeatts, 2000; Bormann, 1992).

On Tinian, USGS investigations show that the maximum lens thickness is approximately 12 meters (40 feet) in the

center of the Median Valley, with slight thinning near the Municipal Well and Marpi Marsh (Gingerich and Yeatts, 2000). The Municipal Well (a Maui-type, infiltration well) supplies the majority of the islands water needs at a rate of approximately 4.5 x 10^6 liters/day (~1.2 Mgal/day). Today water produced from the Municipal well has a chloride concentration of 180 mg/L, which is 100 mg/L greater than when the well was constructed in 1945. The USGS monitored the aquifer thickness in relation to rain events in the wet season of 1993 and reported an aquifer thickening of 90-150 cm (3-5 ft), while reports in the dry season of 1994 showed an aquifer thinning of 30-60 cm (1-2 ft). These results revealed that annual fluctuations are minor and lens thickness is dependent more upon long-term rainfall patterns instead of annual fluctuations, for maintaining overall morphology (Gingerich and Yeatts, 2000). This stable lens morphology indicates that contamination problems have the potential to produce long term effects due to long residence time for water within the aquifer.

With the stable fresh-water lens morphology on Tinian, the location and identification of karst features becomes important for preventing groundwater contamination. Understanding the spatial distribution and extent of fissure caves, pit caves, and recharge features, which can transport contaminants rapidly to the lens, may enable government planners to regulate activities near sensitive areas. Similarly, identified discharge features can be used as sampling points for monitoring possible groundwater contamination. Identification of allogenic recharge may be used to predict regions where parabasal waters may be thicker due to increased recharge, such that salt-water intrusion risks from water extraction may be reduced. Spatial distributions of flank margin and banana hole caves may provide insight into the diffuse flow characteristics of previous fresh-water lenses, making it possible to better evaluate current lens morphology. If positive correlations do exist between brittle deformation and megaporosity, then regional structure may provide insights into groundwater behavior.

STUDY METHODOLOGY

This study had three objectives. It was initially developed to inventory, survey, and classify the cave and karst features on Tinian and Aguijan, because no such database existed for the islands. In addition to the inventory, this study was developed to evaluate whether or not a statistical comparison could be made between megaporosity and zones of brittle failure in eogenetic rocks on carbonate islands, using data collected from the island of Tinian where basic geologic studies have been conducted (Doan et al., 1960). The study was conducted in five major phases, in order to reach the two objectives: 1) initial site investigation, 2) data collection, 3) data reduction, 4) statistical comparison of data, and 5) small-scale test site evaluation. Results from the two primary objectives of the study were used to evaluate the islands of Tinian and Aguijan in relation to the Carbonate Island Karst Model.

INITIAL SITE INVESTIGATION

The initial site investigation included a reconnaissance of Tinian and analysis of the physiography and geology of the island. The reconnaissance was conducted in June 2002 (Stafford et al., 2002) and provided basic information about the cultural, physical and logistical aspects of Tinian, while establishing relationships with local government bodies that would be crucial for in-depth studies on the island. During this reconnaissance areas that were reported by island residents as having significant cave development were visited, including, but not limited to: Suicide Cliffs, Unai Dangkolo,

and Mount Lasu. This initial site investigation demonstrated that most known caves, reported by local residents and hunters, occur predominantly along scarps, coastlines, and closed depressions, which agreed with previous investigations on carbonate islands (Stafford et al., 2002; Mylroie et al., 1999).

After the initial reconnaissance, the islands geography and geology were analyzed with a geographical information system (GIS) that was produced for the island using ArcView 3.2 (ESRI, 2000). A digital elevation model (DEM) was created for the island using spatial data transfer standard (SDTS) compliant raster data with 10-meter postings produced by the National Mapping Program of the United States Geological Survey (USGS, 2001a,b,c,d,e), which provides greater resolution than the 1:25,000 topographic map produced by the USGS (USGS, 1983). The DEM was then overlain with a scanned geology map produced by Doan and coworkers (1960). It was geo-referenced using Image Analyst (ESRI, 2000) in order to scale and align the geology map with DEM, then all igneous outcrops and faults were manually digitized in order to create shape files of these features. The DEM and digitized geologic features were then used as the basic dataset needed to delineate prominent scarps and closed depressions on the island.

Scarps were defined as any change in slope greater than twenty degrees, which enabled the identification of all major scarps in the island interior and coastline (Figure 19, Appendix A). Because of the DEM cell size, smaller scarps that might contain cave entrances were excluded; however, it did not eliminate investigations of smaller coastal scarps because coastlines were identified as sites of cave development during the initial reconnaissance. Closed depressions were defined as regions that were lower than the surrounding topography on all sides. Only closed depressions greater than 10 meters in diameter could be identified based on the limitations of the DEM grid size. The closed depressions where analyzed in relation to outcrops of igneous rock. The closed depressions that were found to be proximal to the igneous outcrops were identified as locations of possible allogenic recharge developed by dissolution, while the closed depressions that were distal to the igneous outcrops probably had non-dissolutional (i.e. constructional or human modified) origin (Figure 20, Appendix A).

The reconnaissance and GIS investigation of Tinian provided a framework for fieldwork and data collection on Tinian. Because there is little published geology on Aguijan and a reconnaissance visit was not possible, no detailed fieldwork plan could be developed. However, this project extended the cave and karst inventory to Aguijan when the opportunity for access to the island was available.

DATA COLLECTION

Two types of data were collected during fieldwork: 1) cave and karst surveys, and 2) structural orientations of zones of brittle failure. These two datasets were collected over the course of two intensive field seasons (December 10, 2002 to January 07, 2003 and May 04, 2003 to June 1, 2003) and provided the database for analysis and correlation in this study. During the course of fieldwork, coastal and scarp investigations were limited to regions that could be accessed within an acceptable risk level that would not greatly endanger safety.

Cave and karst surveys were conducted on Aguijan and Tinian based on the initial site investigation and additional reports provided by local residents during the course of fieldwork. This fieldwork focused on known caves, coastlines, scarps, and closed depressions. Caves were surveyed in accordance with current international standards for cave cartography and mapping established by the National Speleological Society (NSS) (Dasher, 1994) and the Association for Mexican Cave Studies (AMCS) (Sprouse and Russell, 1980). Individual surveys were conducted using a Suunto compass, Suunto inclinometer, and fiberglass tape, in association with a field

sketch recorded by experienced project sketchers. Caves and other karst features, including discharge and recharge features, which did not warrant survey, were photo-documented and recorded. Discharge volumes on discharge features were estimated (minimal discharge and significant discharge), because coastal conditions did not allow for measurements of salinity and temperature to be taken at most sites.

During fieldwork, features were classified by cave type based on their appearance in accordance with the Carbonate Island Karst Model. The feature types included: banana hole, discharge cave/feature, fissure cave, flank margin cave, recharge cave/feature, and pit cave. When satellite coverage permitted, Universal Transverse Mercator System (UTM) coordinates and elevation were recorded with the global positioning system (GPS), in order to establish accurate location information for the feature. When satellite coverage was not possible, because of vegetation or topography, cave locations were identified on 1:25,000 USGS topographic maps (USGS, 1983), which were then used to determine UTM coordinates and elevation for features.

Structural orientations of planes of brittle failure were measured using a Suunto compass during fieldwork on Tinian. Aguijan was excluded from this phase of data collection, because no published geologic map for the island exists and available time on the island was limited. Orientations were taken in areas where a joint or fracture could be observed in the bedrock and was not obscured by karren or phytokarst development. Orientations were only taken where the joint or fracture continued over a distance of several meters, cut through more than one bedding plane or several meters of bedrock, and in areas where the bedrock appeared to be *in situ*.

DATA REDUCTION

Data reduction included five phases: 1) survey data reduction and production of maps of the cave and karst features surveyed on Aguijan and Tinian, 2) analysis of cave maps and delineation of primary cave orientations and cave segment orientations for features on Tinian, 3) analysis of faults and joints reported by Doan and coworkers (1960), 4) analysis of scarp and coastline orientations on Tinian, and 5) orientation data reduction and production of rose diagrams for structural and cave orientations on Tinian.

Data from surveyed cave and karst features was reduced using the software package WALLS (McKenzie, 2002), which enables compass, inclinometer and tape measurements taken during surveys to be plotted with corrections for minor loop closure errors and regional magnetic declination. The corrected line plots for each cave were then used as a basis for drafting spatially correct final maps of the features using Corel Xara 2.0 (Xara, 1997). Final cartographic products were created by overlaying field sketch notes and corrected line plots. The field sketch notes were scaled and rubber-banded to match the corrected line plots, then features recorded on the field sketch notes were manually digitized using standard cave symbology established by the NSS and AMCS (Figure 21, Appendix A; Sprouse and Russell, 1980) in order to create accurate maps of the cave and karst features inventoried.

These maps were used to delineate primary cave orientations and segment orientations for features surveyed on Tinian, using two methods: 1) apparent trends and 2) entrance oriented trends. Cave orientations have been used in previous studies in continental settings to correlate cave and karst development with regional structure (Nelson, 1988; Barlow and Ogden, 1982), where the orientations of individual cave segments that have a consistent trend are measured and compared against regional brittle failure features to determine if a correlation between the two populations exist.

Using the apparent trend method, all Tinian cave maps were analyzed individually and a primary axis was defined

through the cave based on the maximum length of the cave and the location of the breached entrance. Cave segments were then defined by the orientation of individual chambers, passages, and wall characteristics such as large pockets and chamber alcoves (Figures 9 and 10). This technique is highly subjective, but was used because of its similarity to studies in caves where passages tend to be linear (Nelson, 1988; Barlow and Ogden, 1982). The primary and segment cave trends were then measured and compiled. The segment cave trends were length-weighted into 5 and 10-meter increments, such that each 5 or 10-meter section of cave segment was counted as an individual orientation measurement in order to give greater significance to longer segment trends during data analysis (Nelson, 1988; Barlow and Ogden, 1982). Two segment lengths were used to form two sets of data that would reduce the subjectivity of the parameters that were used to define segment length, such that smaller cave sections would be included in the 5-meter segment data, while only larger cave sections would be included in the 10-meter segment data.

The entrance width trend method of delineating cave orientations was developed and performed in an attempt to reduce the subjectivity in data reduction for flank margin and banana hole type caves, which tend to form globular or elliptical chambers instead of the more linear passages seen in fissure caves. Using the entrance orientation method, up to three orientations were measured for flank margin and banana hole type cave maps on Tinian (Figure 11). In this technique, the orientation of the entrances to caves that were entered horizontally was measured. Next a maximum penetration measurement was calculated near perpendicular to the entrance ($90^o \pm 15^o$ from the entrance orientation). In caves that had been breached by ceiling collapse and were entered vertically, no entrance orientation was measured, but the penetration measurement was defined as the longest dimension of the cave. Based on the

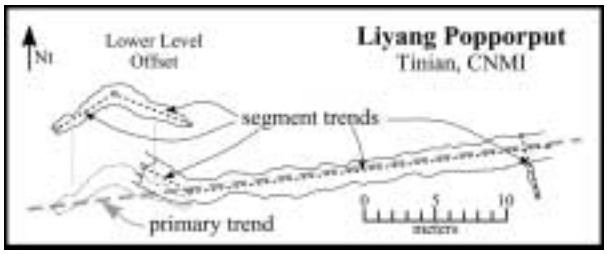

Figure 9: Example of primary and segment orientation trends measured using the apparent trend method for a typical fissure cave.

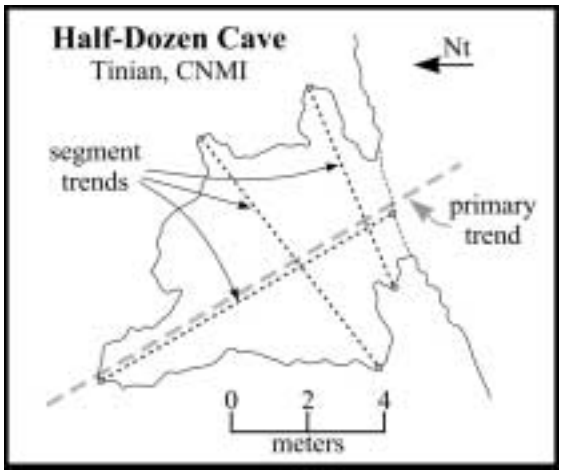

Figure 10: Example of primary and segment orientation trends measured using the apparent trend method for a typical mixing zone cave.

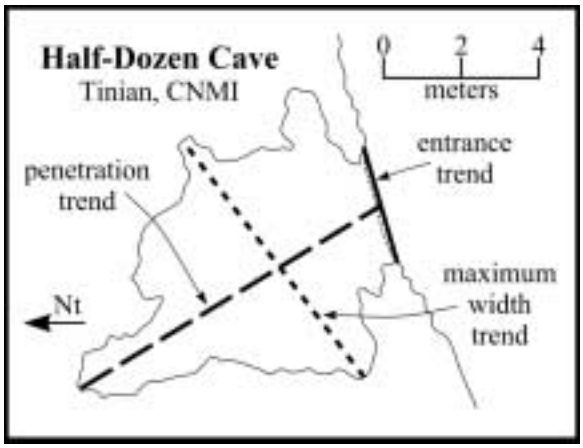

Figure 11: Example of entrance, maximum width, and penetration trends measured using the entrance width trend method for a typical mixing zone cave.

penetration measurement, a maximum width was measured near perpendicular to the penetration orientation ($90^o \pm 15^o$ from the penetration orientation). In cases where the cave entrance was the maximum width, the same measurement was reported for both entrance width and the maximum width. These measurements were then compiled as primary entrance width, penetration length, and maximum width orientations and corresponding segment orientations that were length-weighted in 5 and 10-meter segments similar to the cave segments defined in the apparent method.

Faults and joints reported by Doan and coworkers (1960) were measured for length and orientation. The data for faults was length-weighted by 50 and 100-meter segments in order to apply greater significance to faults that extended over greater distances. Two segment lengths were used in order to reduce the subjectivity in selecting segment lengths, such that shorter lengths would be included in the 50-meter segment data and only longer segments would be included in the 100-meter segment data. These two segment lengths were defined because they are proportional to the segment definition used for cave passages, but measured at a scale that is one order of magnitude greater, because 5 and 10-meter lengths could not be accurately measured from the geology reported by Doan and coworkers (1960). Similarly, all scarps that were identified during the initial site investigation and all coastlines were divided into linear segments in order to eliminate the effects of minor variations in coastal erosion and mass wasting. The linear segments were measured for orientation and length; with length weighted, 50 and 100-meter segments applied to both scarp and coastline orientations as was defined for fault segments, because the DEM cell size does not allow for accurate measurements less than 10 meters.

In the final phase of data reduction, all orientation measurements were reduced to produce rose diagrams using the software package GEOrient 9.2 (Holcombe, 2003), using five-degree orientation sectors in order to be able to visually compare the orientation patterns of caves, zones of brittle failure, scarps, and coastlines. Rose diagrams were produced for each type of orientation data in each of the five physiographic provinces of Tinian (Central Plateau, Median Valley, Northern Lowland, North-Central Plateau, and Southeastern Ridge) and for the entire island of Tinian (Tinian Composite). These rose diagrams include the following types:

1. fault orientations
2. fault, 5-meter segment orientations
3. fault, 10-meter segment orientations
4. joint orientations
5. orientations of fractures measured during fieldwork
6. inland scarp orientations
7. inland scarp, 5-meter segment orientations
8. inland scarp, 10-meter segment orientations
9. coastal scarp orientations
10. coastal scarp, 5-meter segment orientations
11. coastal scarp,10-meter segment orientations
12. all scarps orientations
13. all scarps, 5-meter segment orientations
14. all scarps, 10-meter segment orientations
15. coastline orientations
16. coastline, 5-meter segment orientations
17. coastline, 10-meter segment orientations
18. fissure cave orientations
19. fissure cave, 5-meter segment orientations
20. fissure cave, 10-meter segment orientations
21. mixing zone cave orientations
22. mixing zone cave, 5-meter segment orientations
23. mixing zone cave, 10-meter segment orientations
24. all cave types orientations
25. all cave types, 5-meter segment orientations
26. all cave types, 10-meter segment orientations
27. mixing zone cave penetration orientations
28. mixing zone cave penetration, 5-meter segment orientations
29. mixing zone cave penetration, 10-meter segment orientations

30. mixing zone cave entrance width orientations
31. mixing zone cave entrance width, 5-meter segment orientations
32. mixing zone cave entrance width, 10-meter segment orientations
33. mixing zone cave maximum width orientations
34. mixing zone cave maximum width, 5-meter segment orientations
35. mixing zone cave maximum width, 10-meter segment orientations

STATISTICAL COMPARSION OF DATA

Statistical comparisons were calculated in order to determine if different populations of orientation data were similar within each of the five physiographic provinces of Tinian and the entire island of Tinian. The comparisons were calculated in order to determine if there is a significant relationship between: 1) brittle deformation of eogenetic rocks and the development of eogenetic karst; 2) scarp orientations and the development of eogenetic karst; and 3) coastline orientations and the development of eogenetic karst.

Statistical comparisons were conducted using the Kolmogorov-Smirnov 2-sample test (Burt and Barber, 1996; Till, 1974; Miller and Kahn, 1962), which performs a non-parametric test on two independent sample populations to determine if they represent similar populations or population distributions. During the statistical comparison phase, several populations of orientations were evaluated, which correspond to the 35 orientation types that were used to produce rose diagrams during the data reduction phase. Each of the 35 orientation types was evaluated for correlation with:

1. fault orientations
2. fault, 5-meter segment orientations
3. fault, 10-meter segment orientations
4. joint orientations
5. orientations of fractures measured during fieldwork
6. inland scarp orientations
7. inland scarp, 5-meter segment orientations
8. inland scarp, 10-meter segment orientations
9. coastal scarp orientations
10. coastal scarp, 5-meter segment orientations
11. coastal scarp, 10-meter segment orientations
12. all scarps orientations
13. all scarps, 5-meter segment orientations
14. all scarps, 10-meter segment orientations
15. coastline orientations
16. coastline, 5-meter segment orientations
17. coastline, 10-meter segment orientations

These correlations were performed in order to test three different null hypotheses (H_0):

$H_0(1)$: Regional brittle deformation and karst development represent significantly different populations or population distributions and develop independently.

$H_0(2)$: Regional scarp positions and karst development represent significantly different populations or population distributions and develop independently.

$H_0(3)$: Regional coastline positions and karst development represent significantly different populations or population distributions and develop independently.

The first null hypothesis ($H_0(1)$) was formulated in order to determine if there is a relationship between brittle deformation and karst development on Tinian, while the second and third null hypotheses ($H_0(2$ and $3)$) were formulated to determine if there is a relationship between karst development and coastlines or scarps, where the edge of the paleo fresh-water lens would be expected based on the Carbonate Island Karst Model (Mylroie and Vacher, 1999). Because of the wide variation in orientations of the data in

this study, a high significance level ($P \leq 0.01$) was used to ensure that the populations or population distributions that were compared represented significantly similar datasets. If the first null hypothesis is rejected, then the regional populations of joints, fractures, and faults are similar to the regional karst development and a positive relationship between the two populations can be inferred. If the second null hypothesis is rejected, then the regional populations of scarp orientations are similar to the regional karst development and a positive relationship between the two populations can be inferred. If the third null hypothesis is rejected, then the regional populations of coastline orientations are similar to the regional karst development and a positive relationship between the two populations can be inferred.

SMALL-SCALE TEST SITE EVALUATION

In addition to the analyses performed for the five physiographic provinces and the island of Tinian, smaller-scale test sites were analyzed to determine if any relationships existed at various scales: 1) island scale, 2) province scale, and 3) site scale. Because of the wide distribution of cave and karst features, one square kilometer test sites were chosen for additional analyses. In order to compare the results of analyses from test sites with the larger regions of Tinian, five parameters where required to exist within the one square kilometer boundary, including: 1) three or more surveyed features, 2) both fissure and mixing zone caves, 3) coastline, 4) faults reported by Doan and coworkers (1960), and 5) fracture orientations measured during fieldwork.

The requirements for choosing small-scale test sites required the completion of fieldwork and the cave and karst inventory of this study. Once the inventory stage was complete, three test sites were chosen for analysis (Figure 22, Appendix A): Carolinas Limestone Forest, Puntan Diapblo, and Unai Dangkolo. At each of these sites, statistical comparisons were evaluated using the Kolmogorov-Smirnov 2-sample test, with the same 35 parameters evaluated for each of the physiographic provinces and the entire island of Tinian.

STUDY RESULTS

CAVE AND KARST INVENTORY

The mapping portion of cave and karst inventory surveyed 114 caves or cave complexes (green areas, Figure 23, Appendix A; Appendix B): 26 on Aguijan and 88 on Tinian. The features were classified by morphology type and grouped by physiographic province they were found in (Table 1, Appendix B; Table 2, Appendix B). On Aguijan, the cave survey produced maps of 1 banana hole, 5 fissure caves, and 20 flank margin caves. On Tinian, the cave survey produced maps of 3 banana holes, 5 discharge features, 12 fissure caves, 65 flank margin caves, 1 pit cave, and 2 recharge features; however, 4 of the discharge features were also classified as fissure caves, making a total of 16 fissure caves. Mixing zone type caves (banana hole and flank margin type caves) were the most prominent cave types found during the inventory (81% on Aguijan; 77% on Tinian). While Tinian exhibited a larger diversity and quantity of caves, the ratio of fissure caves to mixing zone caves on both islands was 0.24 (0.235 for Aguijan; 0.238 for Tinian), with fissure caves accounting for almost 20% of the caves recorded.

A total of seventeen locations were found on Tinian, which exhibited fresh-water discharge (Figure 24, Appendix A). Most of these features were identified by schlieren mixing at the coastline, but only five of them were associated with cave development and surveyed. Fresh-water discharge observed at Unai Dangkolo, Unai

Masalok and Taga Beach appeared as diffuse discharge through carbonate sand beach deposits, while the discharge at other sites appeared as focused discharge along fractures and bedding planes. The two discharge features that exhibited the greatest discharge were located on the east and west coasts of the island at Gecko Cave and Barcinas Cove, respectively.

Investigation of closed depressions identified four definite regions of allogenic recharge in the North-Central Highland, with small caves associated with two of them (Lasu Recharge Cave and West Lasu Depression Cave). The presence of accumulated detritus and the lack of sediment coatings on the feature walls is evidence that recharge is rapid and that water does not pond at these features during recharge events. The other two recharge features (North and South Lemmai Recharge Features) covered larger areas, contained contacts between carbonate and non-carbonate rocks, and showed vegetative evidence of water ponding within the closed depressions prior to entering the subsurface (Figure 25, Appendix A). Ponded water was present in portions of South Lemmai Recharge Feature when investigated (Figure 26, Appendix A).

The other sixteen closed depressions identified during the initial site investigation that were not confirmed as allogenic recharge features were also investigated (Figure 27, Appendix A), either physically or through communication with local residents. Five closed depressions were identified as quarries or borrow pits, eight were identified as natural constructional features, and three appear to be recharge features. Four of the modified closed depressions (quarries and borrow pits) showed evidence of excavation in the past, while the quarry located near Barcinas Cove is being actively excavated today (Figure 28, Appendix A). The eight natural construction features showed no evidence of excavation or allogenic recharge; however, Hagoi in the Northern Lowland is less than 2 meters above mean sea-level and contained fresh-water at the time of survey (Figure 29, Appendix A), while the largest closed depression on the island (Sisonyan Makpo) is less than 3 meters above mean sea-level at its lowest elevation and is the site of the islands primary municipal well (Makpo Wells). The three unconfirmed recharge features are located north of Mount Lasu near small outcrops of non-carbonate rocks, but due to their small size and dense vegetation in the area, a positive confirmation could not be made.

CAVE ORIENTATIONS

The two methods of cave orientation analysis (apparent trend and entrance width trend) were applied to orientation data for mapped caves on Tinian. Aguijan was excluded from this analysis because no geologic map has been published for the area, which would compliment the cave orientation data when comparing cave and karst development to brittle failure features. Each cave was analyzed separately, including those that occurred on maps where a complex or series of caves were surveyed together as one map, making it possible to have several datasets of orientation measurements for some cave maps. Using the apparent trend method all fissure caves and mixing zone caves (flank margin and banana hole type caves) were analyzed for primary orientation and segment orientations. The single pit cave and two recharge caves were excluded from all datasets except composite cave types (all cave types) because of their small sample size. Using the entrance trend method, the mixing zone caves were analyzed for entrance width, penetration length and maximum width, while fissure caves, the single pit cave and the two recharge caves were excluded. The fissure caves were excluded from the entrance width trend method because they are linear features with distinct segment orientations similar to telogenetic caves (Nelson, 1988; Barlow and Ogden, 1982), while the single pit cave and two recharge caves were excluded again because of their small sample size.

The apparent trend method was applied because of its similarity to previous studies (Nelson, 1988; Barlow and Ogden, 1982). Apparent trend analysis of fissure caves analysis yielded 18 primary cave orientations (Table 3, Appendix C): 5 in the Central Plateau; 5 in the Median Valley; 0 in the North-Central Highland; 1 in the Northern Lowland; and 7 in the Southeastern Ridge. Fissure cave segment analysis using the apparent trend method yielded 147 orientations with 297 five-meter segments and 135 ten-meter segments (Table 4, Appendix C):

- Central Plateau: 15 orientations, 24 five-meter segments and 12 ten-meter segments
- Median Valley: 69 orientations, 100 five-meter segments and 44 ten-meter segments
- North-Central Highland: 0 orientations and segments
- Northern Lowland: 2 orientations, 2 five-meter segments and 2 ten-meter segments
- Southeastern Ridge: 61 orientations, 171 five-meter segments and 77 ten-meter segments

Apparent trend analysis of mixing zone caves yielded 128 primary orientations (Table 5, Appendix C): 46 in the Central Plateau; 27 in the Median Valley; 8 in the North-Central Highland; 1 in the Northern Lowland; and 46 in the Southeastern Ridge. Mixing zone cave segment analysis yielded 388 orientations with 980 five-meter segments and 480 ten-meter segments (Table 6, Appendix C):

- Central Plateau: 123 orientations, 302 five-meter segments and 122 ten-meter segments
- Median Valley: 126 orientations, 424 five-meter segments and 212 ten-meter segments
- North-Central Highland: 20 orientations, 30 five-meter segments and 9 ten-meter segments
- Northern Lowland: 4 orientations, 11 five-meter segments and 9 ten-meter segments
- Southeastern Ridge: 115 orientations, 213 five-meter segments and 128 ten-meter

The entrance width trend method was performed in order to reduce the subjectivity of orientation measurements that exist in the apparent trend method. Measurements used in the entrance width trend method included entrance width, penetration length, and maximum width, with 10 caves excluded from the entrance width analysis because their entrances were entered vertically as a result of ceiling collapse. Entrance width analysis using the entrance trend method yielded 107 entrance widths with 324 five-meter segments and 163 ten-meter segments (Table 7, Appendix C):

- Central Plateau: 40 orientations, 105 five-meter segments and 59 ten-meter segments
- Median Valley: 20 orientations, 89 five-meter segments and 43 ten-meter segments
- North-Central Highland: 5 orientations, 11 five-meter segments and 6 ten-meter segments
- Northern Lowland: 1 orientation, 22 five-meter segments and 11 ten-meter segments
- Southeastern Ridge: 42 orientations, 97 five-meter segments and 44 ten-meter segments

Penetration length analysis using the entrance trend method produced 118 orientations with 369 five-meter segments and 190 ten-meter segments (Table 8, Appendix C):

- Central Plateau: 42 orientations, 116 five-meter segments and 54 ten-meter segments
- Median Valley: 26 orientations, 116 five-meter segments and 67 ten-meter segments
- North-Central Highland: 6 orientations, 15 five-meter segments and 6 ten-meter segments
- Northern Lowland: 1 orientation, 16 five-meter segments and 8 ten-meter segments

- Southeastern Ridge: 43 orientations, 106 five-meter segments and 55 ten-meter segments

Maximum width analysis using the entrance trend method yielded 118 orientations with 407 five-meter segments and 208 ten-meter segments (Table 9, Appendix C):

- Central Plateau: 42 orientations, 140 five-meter segments and 72 ten-meter segments
- Median Valley: 26 orientations, 116 five-meter segments and 60 ten-meter segments
- North-Central Highland: 6 orientations, 13 five-meter segments and 7 ten-meter segments
- Northern Lowland: 1 orientation, 22 five-meter segments and 11 ten-meter segments
- Southeastern Ridge: 43 orientations, 116 five-meter segments and 58 ten-meter segments

BRITTLE DEFORMATION

Analysis of the data from the geologic survey conducted by Doan and coworkers (1960) identified 313 faults (Figure 30, Appendix A) and 112 joints on Tinian. The data reported by Doan and coworkers (1960) was divided by physiographic province and measured separately, with faults that occurred at the boundary between two physiographic provinces not being reported, because Doan and coworkers (1960) defined the five physiographic provinces based on high-angle faults that divided the island into distinct regions. The measurements for each of the faults were length weighted to produce a total of 3322 fifty-meter segments and 1661 one hundred-meter segments with segments rounded to the nearest 50 and 100-meter increment. This process produced 39 orientations with 358 fifty-meter segments and 179 one hundred-meter segments in the boundary areas separating different physiographic provinces (Table 10, Appendix C), which included:

- Central Plateau: 94 orientations, 944 fifty-meter segments and 472 one hundred-meter segments
- Median Valley: 50 orientations, 686 fifty-meter segments and 343 ten-meter segments
- Northern Lowland: 22 orientations, 324 fifty-meter orientations and 162 ten-meter segments
- North-Central Highland: 43 orientations, 394 fifty-meter segments and 197 one hundred-meter segments
- Southeastern Ridge: 65 orientations, 618 fifty-meter segments and 309 one hundred-meter segments

Joint data reported by Doan and coworkers (1960) produced 38 orientations in the Central Plateau, 25 orientations in the Median Valley, 0 orientations in the North-Central Highland, 16 orientations in the Northern Lowland, and 33 orientations in the Southeastern Ridge (Table 11, Appendix C).

Measurements of planes of brittle failure measured during fieldwork yielded 345 orientations for the island of Tinian (Table 12, Appendix C). Because of dense vegetation, soil cover, and the criteria used for orientation sampling, the orientations measurements were primarily limited to coastal areas where exposed bedrock could be observed. However, measurements were attained in all regions accept the North-Central Highland, which has no coastline. Measurements included 103 orientations in the Central Plateau, 106 orientations in the Median Valley, 86 orientations in the Northern Lowland, and 50 orientations in the Southeastern Ridge.

SCARPS AND COASTLINES

Analysis of scarps based on 20-degree slopes derived from the ten-meter posting DEM provided the basis for scarp orientations on Tinian (Figure 19, Appendix A). Scarps were divided into inland scarps and coastal scarps and measured, resulting in a total of 154 inland scarp orientations with 725 fifty-meter segments and 379 one hundred-meter segments and 147 coastal

scarp orientations with 539 fifty-meter segments and 266 one hundred-meter segments (Tables 13 and 14, Appendix C). The measurements were grouped by the physiographic province for both the inland and coastal scarps for data analysis. Inland scarp orientations included (Table 13, Appendix C):

- Central Plateau: 27 orientations, 126 fifty-meter segments and 68 one hundred-meter segments
- Median Valley: 12 orientations, 46 fifty-meter segments and 24 one hundred-meter segments
- North-Central Highland: 30 orientations, 150 fifty-meter segments and 79 one hundred-meter segments
- Northern Lowland: 0 orientations
- Southeastern Ridge: 85 orientations, 403 fifty-meter segments and 208 ten-meter segments

Coastal scarp orientations included (Table 14; Appendix C):

- Central Plateau: 65 orientations, 539 fifty-meter segments and 101 ten-meter segments
- Median Valley: 3 orientations, 10 fifty-meter segments and 5 one hundred-meter segments
- North-Central Highland: 0 orientations
- Northern Lowland: 0 orientations
- Southeastern Ridge: 79 orientations, 320 fifty-meter segments and 160 one hundred-meter segments

Coastline orientations were measured at the 0 elevation contour on the DEM for Tinian. Coastlines were measured similar to island scarps, producing 251 orientations with 945 fifty-meter segments and 501 one hundred-meter segments for the island (Table 15, Appendix C), which yielded 50.1 kilometers of coastline segments, closely approximating the 51.2 kilometers of coastline that exist (Doan et al., 1960). The coastline measurements were grouped by the appropriate physiographic province, with:

- Central Plateau: 84 orientations, 250 fifty-meter segments and 134 one hundred-meter segments
- Median Valley: 48 orientations, 169 fifty-meter segments and 94 one hundred-meter segments
- Northern Lowland: 40 orientations, 206 fifty-meter segments and 113 one hundred-meter segments
- Southeastern Ridge: 79 orientations, 320 fifty-meter segments and 160 one hundred-meter segments

The North-Central Plateau is surrounded on all sides by other physiographic provinces and has no coastline.

ROSE DIAGRAMS

Rose diagrams were plotted for each of the 35 parameters investigated in this study, with diagrams corresponding to each of the physiographic provinces and the entire island of Tinian (Appendix C). The data was visually analyzed to determine if any similar populations or population distributions existed between independent parameters within the same region. The orientation data showed a wide range of variability, while some datasets contained no orientations or only one orientation trend, which eliminated them from the comparison. The rose diagrams for the Central Plateau and the Northern Lowland showed no distinct similarities, while the diagrams for the entire island of Tinian, Median Valley, North-Central Highland, and Southeastern Ridge showed few distinct similarities.

The data for the entire island of Tinian (Tinian Composite) showed similarity in four parameter comparisons:

1. inland scarp orientations and 10-meter segment orientations of mixing zone cave entrance widths
2. 50-meter segment orientations of inland scarps and 10-meter segment orientations of mixing zone cave entrance widths
3. 100-meter segment orientations of inland scarps and 10-meter segment orientations of mixing zone cave entrance widths

4. 100-meter segment orientations of coastal scarps and mixing zone entrance width orientations

The data for the Median Valley showed similarity in three parameter comparisons:

1. orientations of fractures measured in the field and 5-meter segment orientations of mixing zone cave entrance widths
2. orientations of fractures measured in the field and 10-meter segment orientations of mixing zone cave entrance widths
3. composite scarp orientations and mixing zone cave entrance width orientations

The data for the North-Central Highland showed similarity in three parameter comparisons:

1. inland scarp orientations and composite cave primary orientations
2. inland scarp orientations and mixing zone cave primary orientations
3. composite scarp orientations and composite cave primary orientations

The data for the Southeastern Ridge showed similarity in 13 parameter comparisons:

1. fault orientations and composite cave primary orientations
2. fault orientations and 10-meter segment orientations of mixing zone cave penetrations
3. 50-meter segment orientations of faults and composite cave primary orientations
4. 50-meter segment orientations of faults and 5-meter segment orientations of mixing zone cave penetrations
5. 50-meter segment orientations of faults and 10-meter segment orientations of mixing zone cave penetrations
6. 100-meter segment orientations of faults and composite cave primary orientations
7. 100-meter segment orientations of faults and 5-meter segment orientations of mixing zone cave penetrations
8. 100-meter segment orientations of faults and 10-meter segment orientations of mixing zone cave penetrations
9. orientations of fractures measured in the field and 10-meter segment orientations of mixing zone caves
10. 50-meter segment orientations of inland scarps and 10-meter segment orientations of mixing zone cave entrance widths
11. 100-meter segment orientations of inland scarps and 10-meter segment orientations of mixing zone cave entrance widths
12. coastal scarp orientations and 5-meter segment orientations of mixing zone cave maximum widths
13. coastline orientations and 5-meter segment orientations of mixing zone cave maximum widths

STATISTICAL COMPARISON

Orientation datasets were compared for population similarities or population distribution similarity by performing non-parametric tests on independent samples for each of the physiographic regions and the island of Tinian. Populations or population distributions were considered similar if the significance level between two independent samples was less than 0.01 ($P \leq 0.01$) when compared using the Kolmogrov-Smirnov 2-sample test. The data showed a high degree of similarity with results varying for each province and the island of Tinian.

Tinian Composite

Statistical comparisons for the entire island of Tinian showed similarity for 266 (60.2 %) pairs of independent data. Joints and fracture orientations measured in the field were similar to the faults, while segment datasets showed similarity to all segment lengths in 37 dataset comparisons (Table 16; Appendix D):

1. faults and inland scarps
2. faults and all scarps
3. faults and coastlines
4. faults and all cave types
5. faults and fissure caves
6. faults and mixing zone caves
7. faults and mixing zone cave penetrations
8. faults and mixing zone cave entrance widths
9. faults and mixing zone cave maximum widths
10. inland scarps and all cave types
11. inland scarps and fissure caves
12. inland scarps and mixing zone caves

13. inland scarps and mixing zone cave penetrations
14. inland scarps and maximum cave widths
15. coastal scarps and all cave types
16. coastal scarps and fissure caves
17. inland scarps and mixing zone caves
18. inland scarps and mixing zone cave penetrations
19. inland scarps and mixing zone cave entrance widths
20. inland scarps and mixing zone cave maximum widths
21. coastal scarps and all cave types
22. coastal scarps and fissure caves
23. coastal scarps and mixing zone caves
24. coastal scarps and mixing zone cave penetrations
25. coastal scarps and mixing zone cave entrance widths
26. coastal scarps and mixing zone cave maximum widths
27. all scarps and coastlines
28. all scarps and all cave types
29. all scarps and fissure caves
30. all scarps and mixing zone caves
31. all scarps and mixing zone cave penetrations
32. all scarps and mixing zone cave entrance widths
33. all scarps and mixing zone cave maximum widths
34. coastlines and all cave types
35. coastlines and fissure caves
36. coastlines and mixing zone caves
37. coastlines and mixing zone cave penetration

Central Plateau

Statistical comparisons for the Central Plateau showed similarity for 199 (45.0 %) pairs of independent data. Joints and fracture orientations measured in the field are similar to the faults, while the segment datasets showed similarity for all segment lengths in 19 dataset comparisons (Table 17, Appendix D):

1. faults and inland scarps
2. faults and coastal scarps
3. faults and all scarps
4. faults and all cave types
5. faults and fissure caves
6. faults and mixing zone caves
7. faults and mixing zone cave penetrations
8. faults and mixing zone cave entrance widths
9. faults and mixing zone cave maximum widths
10. inland scarps and coastal scarps
11. inland scarps and all scarps
12. inland scarps and all cave types
13. coastal scarps and all cave types
14. coastal scarps and mixing zone caves
15. coastal scarps and mixing zone cave entrance widths
16. all scarps and mixing zone cave entrance widths
17. coastlines and all cave types
18. coastlines and mixing zone caves
19. coastlines and mixing zone cave entrance widths

Northern Lowland

Statistical comparisons for the Northern Lowland showed similarity for 72 (52.9 %) pairs of independent data. Although only 72 datasets showed similarity, this is more than half of the total comparisons for the province, because data was limited for this region. Analysis of the DEM produced no scarps and the cave and karst inventory only mapped two features (Rogue Cave and Unai Lamlam) in the Northern Lowland. Joints and fracture orientations measured in the field were similar, while segment datasets showed similarity for all segment lengths in eight dataset comparisons (Table 18, Appendix D):

1. faults and all cave types
2. faults and mixing zone cave penetrations
3. faults and mixing zone cave entrance widths
4. faults and mixing zone cave maximum widths
5. coastlines and all cave types
6. coastlines and mixing zone cave penetrations
7. coastlines and mixing zone cave entrance widths
8. coastlines and mixing zone maximum widths

North-Central Highland

Statistical comparisons for the North-Central Highland showed similarity for 12

(7.0 %) pairs of independent data. This province showed the least similarity between orientations datasets for all segment lengths; however, data were limited for the region. Because this province is completely surrounded by other provinces, no coastal scarps or coastlines exist for this province. Additionally, structural data were limited to the faults reported by Doan and coworkers (1960) and no fissure caves were located in this region during fieldwork. Segment datasets showed similarity in only two dataset comparisons (Table 19, Appendix D):

1. faults and inland scarps
2. faults and all cave types

Median Valley

Statistical comparisons for the Median Valley showed similarity for 189 (42.8 %) pairs of independent data. Joints and fractures measured during fieldwork were not similar to the faults for this province, but segment datasets showed similarity for all segment lengths in 27 dataset comparisons (Table 20, Appendix D):

1. faults and inland scarps
2. faults and all scarps
3. faults and all coastlines
4. faults and all cave types
5. faults and mixing zone caves
6. faults and mixing zone cave penetrations
7. faults and mixing zone cave entrance widths
8. faults and mixing zone cave maximum widths
9. inland scarps and coastal scarps
10. inland scarps and coastlines
11. inland scarps and all cave types
12. inland scarps and mixing zone caves
13. inland scarps and mixing zone cave penetrations
14. inland scarps and mixing zone cave entrance widths
15. inland scarps and mixing zone cave maximum widths
16. all scarps and all coastlines
17. all scarps and all cave types
18. all scarps and mixing zone caves
19. all scarps and mixing zone cave penetrations
20. all scarps and mixing zone cave entrance widths
21. all scarps and mixing zone cave maximum widths
22. coastlines and all cave types
23. coastlines and fissure caves
24. coastlines and mixing zone cave types
25. coastlines and mixing zone cave penetrations
26. coastlines and mixing zone cave entrance widths
27. coastlines and mixing zone maximum widths

Southeastern Ridge

Statistical comparisons for the Southeastern Ridge showed similarity for 236 (53.4 %) pairs of independent data. Joints and fractures measured during fieldwork were not similar to the faults for this province, but segment datasets showed similarity for all segment lengths in 23 dataset comparisons (Table 21, Appendix D):

1. faults and all cave types
2. faults and fissure caves
3. faults and mixing zone cave penetrations
4. faults and mixing zone cave entrance widths
5. faults and mixing zone cave maximum widths
6. inland scarps and all cave types
7. inland scarps and fissure caves
8. inland scarps and mixing zone cave penetrations
9. inland scarps and mixing zone cave entrance widths
10. inland scarps and mixing zone cave maximum widths
11. coastal scarps and all cave types
12. coastal scarps and fissure caves
13. coastal scarps and mixing zone cave penetrations
14. coastal scarps and mixing zone cave entrance widths
15. all scarps and all cave types
16. all scarps and fissure caves
17. all scarps and mixing zone cave penetrations
18. all scarps and mixing zone cave entrance widths
19. all scarps and mixing zone cave maximum widths

20. coastlines and all cave types
21. coastlines and fissure caves
22. coastlines and mixing zone cave penetrations
23. coastlines and mixing zone cave entrance widths

SMALL-SCALE TEST SITES

Three one square kilometer tests sites (Figure 22, Appendix A; Carolinas Limestone Forest, Puntan Diapblo, and Unai Dangkolo) were analyzed separately to determine if orientation data from independent populations showed similarity at a smaller scale. Statistical comparisons were made for each of the three test sites using the same criteria as was used for the province and island scale comparisons. As in the larger scale orientation comparisons, datasets were considered to represent similar populations or population distributions if they showed a significance level less than 0.01 ($P \leq 0.01$) when compared using the Kolmogrov-Smirnov 2-sample test. The results of the comparisons for the test sites showed less similarity than the data evaluated over larger regions, but did show significant similarity.

Carolinas Limestone Forest

Statistical comparisons for the Carolinas Limestone Forest test site showed similarity for 64 (18.7 %) pairs of independent data. The test site included three fissure caves (Carolinas Fracture Cave, Plunder Cave, and Water Cave) and one mixing zone cave (Skip Jack Cave). No joint data was reported for this area, but fracture orientations measured in the field showed similarity to faults. Segment datasets showed similarity for all segment lengths in three dataset comparisons (Table 22, Appendix D):

1. faults and all cave types
2. faults and fissure cave
3. faults and mixing zone cave maximum widths

Puntan Diapblo

Statistical comparisons for the Puntan Diapblo test site showed similarity for 67 (16.4 %) pairs of independent data. The test site included three fissure caves (Death Fracture Complex) and nine mixing zone caves (Cavelet Cave, Dos Sakis Cave Complex, Flamingo Tail Cave Complex, Monica Cave, Orange Cave, and Liyang Diapblo). No joint data was reported for the area, but fracture orientations measured in the field showed similarity to faults, inland scarps, all cave types, fissure caves, mixing zone cave entrance widths, and mixing zone cave maximum widths. Segment datasets showed similarity to all segment lengths in two dataset comparisons (Table 23, Appendix D):

1. faults and inland scarps
2. faults and mixing zone cave penetrations

Unai Dangkolo

Statistical comparisons for the Unai Dangkolo test site showed similarity for 63 (44.7 %) pairs of independent data. The test site included one fissure cave (Dripping Tree Fracture Cave) and five mixing zone caves (Andyland Cave, John's Small Cave, Liyang Dangkolo, North and South Unai Dangkolo). No joint data was reported for the area and no scarps could be resolved from the DEM for the area. Fractures measured in the field showed similarity to the coastline, mixing zone cave penetrations, mixing zone cave entrance widths, and mixing zone cave maximum widths. Segment datasets showed similarity to all segment lengths in seven dataset comparisons (Table 24, Appendix D):

1. faults and coastlines
2. faults and mixing zone cave entrance widths
3. faults and mixng zone cave maximum widths
4. coastline and all cave types
5. coastline and fissure caves
6. coastline and mixing zone caves
7. coastline and mixing zone cave penetrations

DISCUSSION AND CONCLUSIONS

TINIAN CAVE AND KARST INVENTORY

The Tinian cave and karst inventory surveyed eighty-eight caves (Figure 23. Appendix A), located seventeen sites of freshwater discharge (Figure 24, Appendix A), and four allogenic recharge areas (Figure 27, Appendix A). Cave development on Tinian is dominated by mixing zone type caves (flank margin and banana hole type caves), but fissure caves account for twenty percent of the total. Only one pit cave and two recharge caves were identified (see Appendix B for maps and descriptions of individual cave and karst features).

The lack of pit caves and recharge caves suggests that these features are uncommon on Tinian; however, it is possible that more exist and that this is a sampling bias. Tinian experienced intense sugarcane farming during the Japanese occupation and extensive military construction by the U. S. and Japan during and after World War Two. If more of these features existed in the past, it is probable that they were infilled intentionally as part of island development or infilled by soil erosion from deforestation, farming and construction. Although soils may be limited in eogenetic karst environments, it is probable that the soil present will erode more easily as a result of human modification of the land surface.

Mixing zone caves were located in every physiographic province and at elevations from sea level to over 150 meters. Three caves were classified as banana holes because they are small features located shallow in the subsurface and are significantly wider than tall; however, these may represent small flank-margin caves. Most coves represent collapsed flank margin caves that have been breached by coastal processes (Figure 31, Appendix A), with speleothems and remnant cave chambers confirming their origin. One feature located north of Unai Dangkolo (Hidden Beach Cave, Figure 32, Appendix A) confirmed that these were collapsed flank margin caves because it was breached at sea level and contained a carbonate sand floor, but retained several regions of intact ceiling rock. Flank margin caves have a wide range of sizes, from a few square meters to the archetypical Tinian flank margin cave (Liyang Dangkolo, Figure 33, Appendix A) that is over 1,300 square meters. Smaller caves have single chambers and larger caves have central chambers with smaller, interconnected passages extending from them (Figure 12), demonstrating how mixing zone caves become interconnected as they grow in size (Figure 13). Horizons of flank margin cave development (Figure 14) occur at several locations, including Mendiola Cove, the southeastern portion of

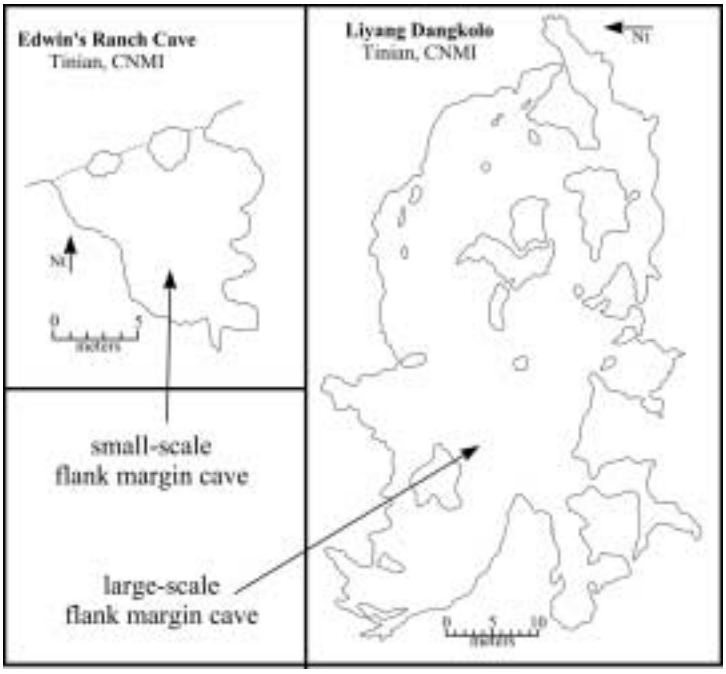

Figure 12: Flank margin caves develop more complicated morphologies as they grow in size as observed on Tinian (note these figures only include bedrock walls and columns in the cave maps).

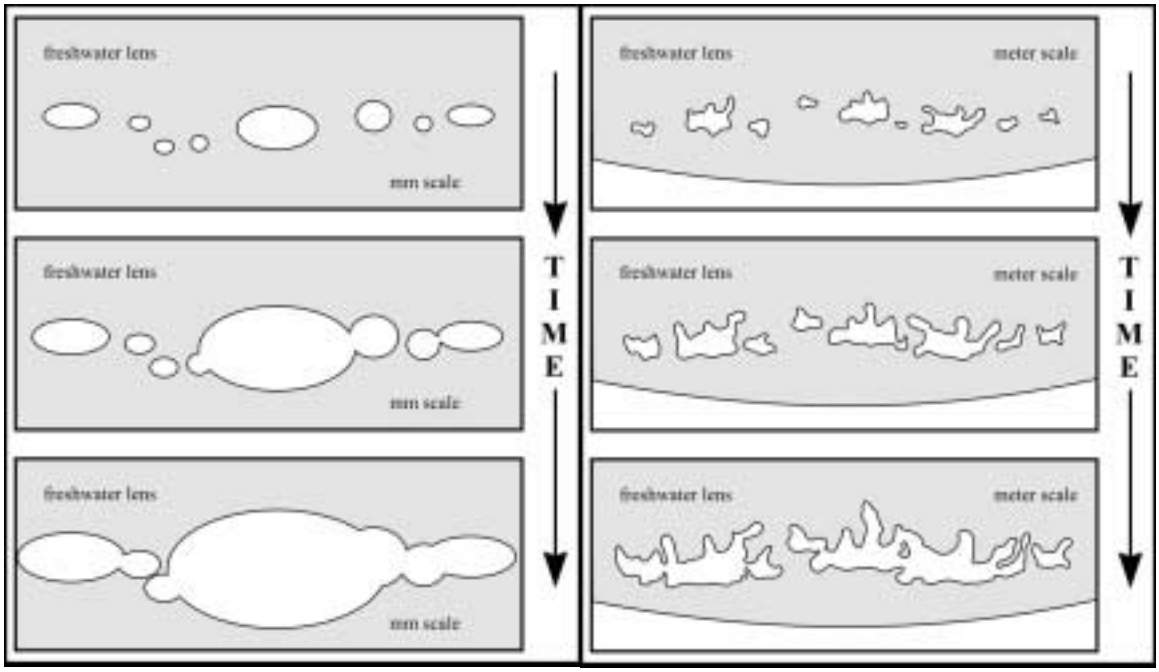

Figure 13: Conceptual model for the growth of flank margin caves. At small scales (vug scale) mixing zone dissolution forms simple ellipse because the rock is locally homogeneous. However, at larger scales (cave scale) inhomogeneities in rock form more complex morphologies with growth as a result of preferential dissolution of the bedrock.

Piña Ridge, Suicide Cliffs, Unai Dangkolo, and Unai Masalok. These horizons indicate at least three previous fresh-water lens positions on Tinian (Figure 34, Appendix A), but complex faulting prevents the direct correlation of horizons of mixing zone development across large regions.

Fissure caves show linear development that appears to be associated with brittle failure (Figure 35, Appendix A). They were located in all physiographic provinces except the North-Central Highland and at elevations ranging from sea level to over 100 meters. These caves can extend to significant depths when located in inland regions and provide fast flow routes for autogenic recharge. The deepest fissure cave (Masalok Fracture Cave) is 42 meters deep and has pools of fresh water at the bottom. Coastal fissure caves generally extend inland at angles near perpendicular to the coastline and frequently have fresh-water discharge associated with them. Other fissure caves (Plunder Cave and Water Cave) form broader, linear, dipping chambers with much collapse and are located near reported faults (Doan et al., 1960). No evidence of offset resulting from faulting could be seen in these caves, either because it does not exist or because extensive flowstone and speleothem development covering the walls obscured it (Figure 36, Appendix A).

Groundwater recharge on Tinian is primarily autogenic. Closed depressions and recharge caves in the North-Central Highland indicate allogenic recharge occurs where volcanic rocks crop out. The small igneous outcrop near the municipal well does not show direct evidence of supplying waters for allogenic recharge, but clays weathered from the volcanic exposure may be armoring the carbonate rock slope below, decreasing the effectiveness of autogenic recharge in these rocks and providing some allogenic recharge to the large closed depression where the municipal well is located. If this is occurring, this allogenic recharge is likely to be minimal because the igneous rocks crop out only on the steep

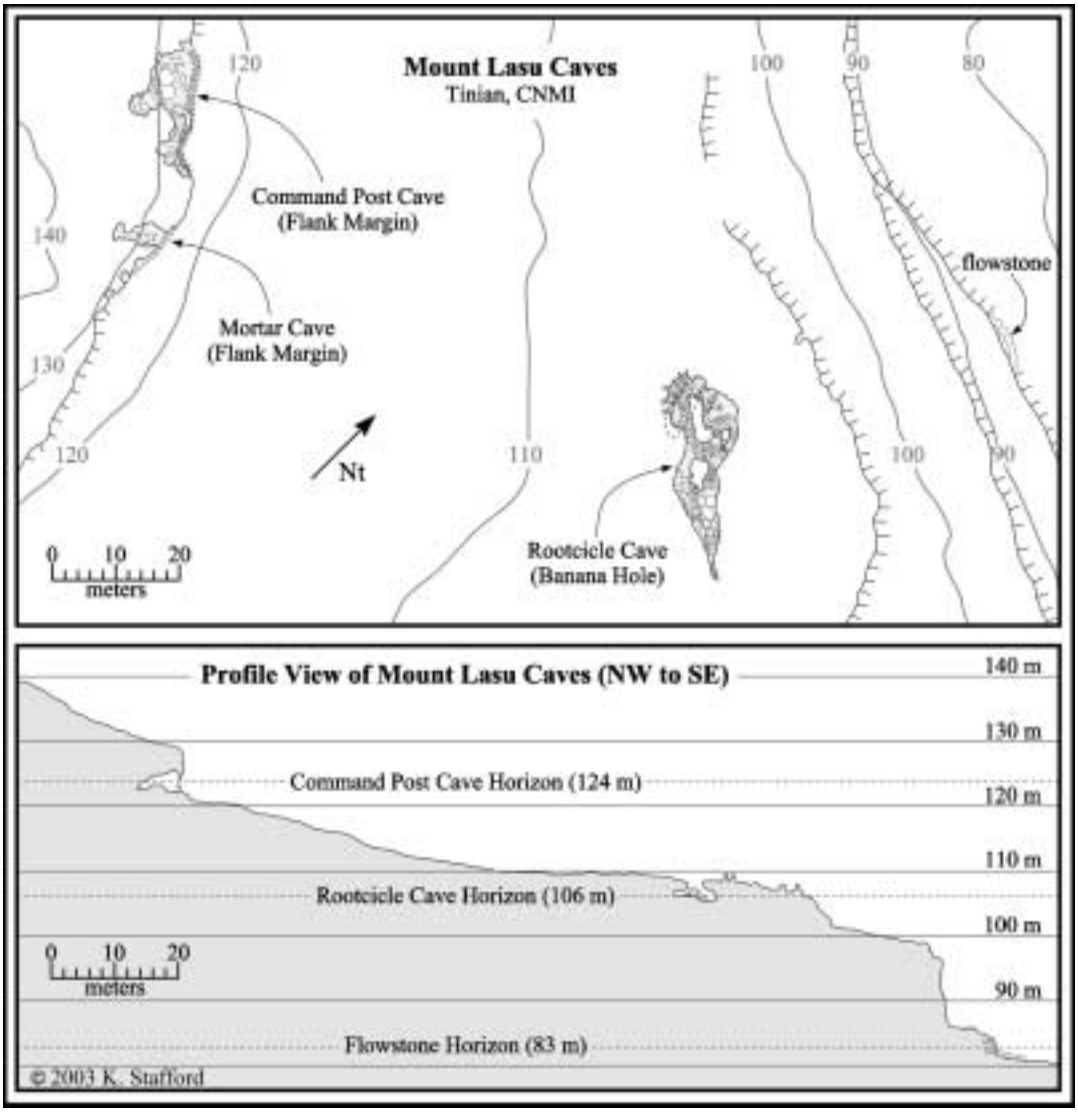

Figure 14: Multiple levels of mixing zone dissolution exist on Tinian with at least three identified in the North-Central Highland near Mount Lasu. However, more probably exist, but island faulting prevents correlation of horizons of development across large regions.

slope over a small area. In addition to the closed depressions that showed evidence of allogenic recharge, five closed depressions were identified as quarries or borrow pits. Although these features have autogenic recharge, recharge rates in these closed depressions is expected to be faster than in other regions of autogenic recharge because the soil cover and surface rock have been removed.

Fresh-water discharge was observed across much of the east and west coast. Much of the coastline could not be investigated due to strong surf; therefore, it is expected that many more discharge sites exist. The discharge sites that were located were generally associated with focused discharge along bedding planes or fractures, indicating that much of the fresh-water discharge is occurring along preferential flow routes, which would be expected to distort the lens morphology regionally. Areas near fissure caves that were discharging fresh-water did not have any

breached flank-margin caves nearby. This may indicate that these features have distorted the fresh-water lens to a great enough degree that the mixing zone caves are not forming in these areas or that they are developing further inland and have not been breached by coastal processes as have other flank margin caves seen along coastlines elsewhere.

AGUIJAN CAVE AND KARST INVENTORY

The cave and karst inventory surveyed 26 features on Aguijan (see Appendix B for maps and descriptions of individual cave and karst features); however, no site of fresh-water discharge was identified because the time was limited on the island and the coastline consists of large scarps that are subject to constant heavy surf. The inventory identified two banana holes, nineteen flank margin caves, five fissure caves, and one problematic cave. According to local guides, these 26 features represent the majority of the caves on Aguijan. The general morphology of Aguijan appears similar to the Carolinas Ridge on Tinian and is expected to have a similar geologic history, although no detailed geologic studies have been conducted on Aguijan to confirm this.

Fissure and mixing zone caves are located at all three terrace levels and on all sides of the island. Boonie Bee Sink may be a small flank margin cave, but because of its general morphology it was classified as a banana hole. The flank margin caves range in size from a few square meters to hundreds of square meters. The fissure caves show three distinct morphologies, which appear to correspond with the morphologies seen on Tinian. Two of the fissure caves (Insect Bat Cave and Toppled Column Cave), located at the edge of the middle terrace, are similar to freshwater discharge caves seen on Tinian and Guam (Taborosi, 2002), but do not discharge freshwater. These two features have been identified as paleo-discharge features (Figure 37, Appendix A).

The one problematic cave (Liyang Atkiya) does not show typical island karst development. It consists of a large entrance chamber, which descends steeply and is floored with breakdown. At the base of this chamber, the walls and floor are coated with a thick coating of dark sediment. The chamber also contains several small pools of water. Extending from the large chamber, a linear passage continues for several hundred meters, while continuing to descend gradually. Old Scallops on the walls of this linear passage indicate that in the past water was flowing upwards from deeper in the cave towards the entrance chamber (Figure 38, Appendix A). The linear passage eventually splits and small mazelike tubes are encountered, which were not completely surveyed. The origin of this feature is problematic because scallops are not normally seen in island karst because of the dominance of mixing zone dissolution. Kalabera Cave on Saipan contains scallops (Jenson et al., 2002), which indicate that water was rising as a lift tube along a lithologic barrier of non-carbonate rocks. However, the lack of evidence of non-carbonate rocks in Liyang Atkiya prevents applying the Kalabera Cave model to this cave. Another investigator sampled black sediments from Liyang Atkiya. Analysis of this material may provide further insight into the origin of this cave.

CONTROLS ON CAVE AND KARST DEVELOPMENT

The second objective of this study is to determine if comparisons of cave development orientation trends to brittle failure trends show similarity that would indicate structural influence on eogenetic karst development or if karst development is related to scarp and coastline positions where the margin of the paleo or current fresh-water lens is expected to be. Cave and karst development in continental settings is significantly influenced by geologic structure and lithology (Klimchouk and Ford, 2000; White, 1988), while island karst is dominated by mixing zone dissolution

with the fresh-water lens position significantly influencing porosity development. Jenson and coworkers (Jenson et al., 2002; Mylroie et al., 2001) have recently recognized the importance of structural and geologic controls on eogenetic, island karst development, but the extent of the influence that geologic structure and lithology have on carbonate island karst development has not been well studied. The morphological difference in fissure caves and mixing zone caves suggests that each class of cave development is dominated by different controls on dissolution. A simple comparison of the length to width ratio for fissure caves and mixing zone caves shows that these two general cave types represent different populations (Figure 15).

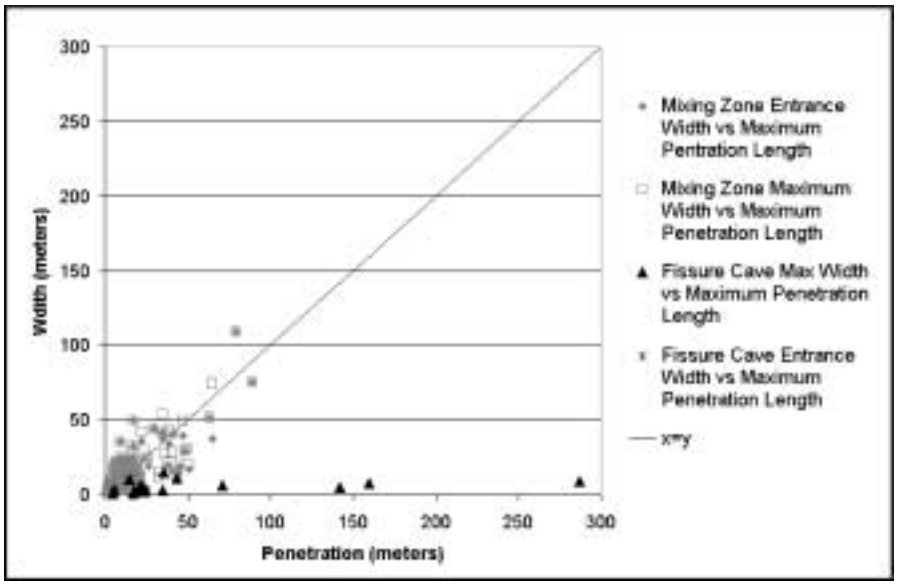

Figure 15: Diagram showing the relationship between cave widths and lengths, which represent two distinct populations for fissure caves and mixing zone caves. Note that as flank margin caves grow in size they have a length to width ratio close to one.

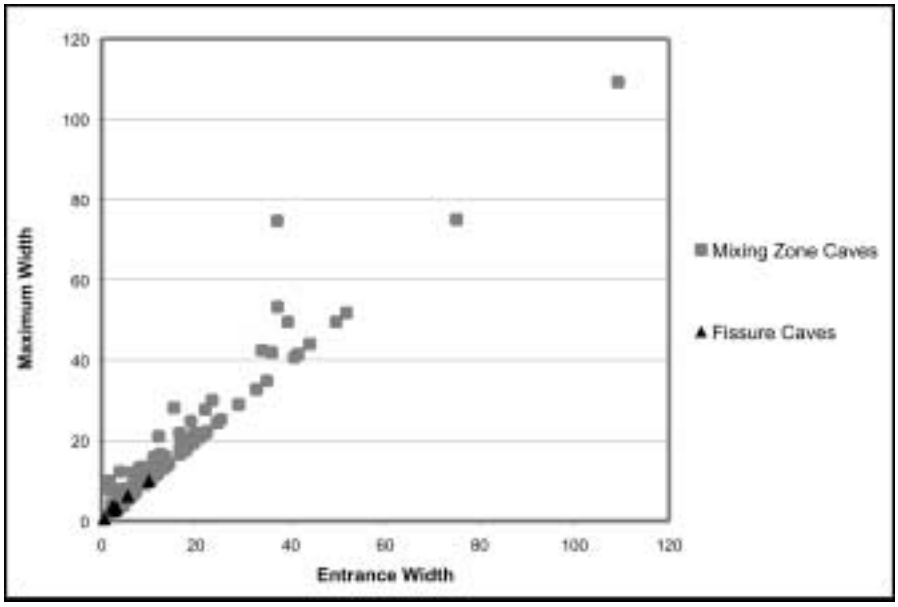

Figure 16: Diagram showing the relationship cave entrance width and cave maximum width. Note that a large portion of the caves plot with a ratio of one, indicating that the entrance width and the maximum width are the same.

This portion of the study was only conducted on data from Tinian, where the geology and structural deformation had been mapped (Doan et al., 1960), because of the focus on the relationship between zones of brittle failure and karst development. Several biases may have been introduced into the data that would affect the results of the comparison of orientation populations. It is inevitable that in the cave and karst

inventory some features were not inventoried because of time constraints in the field, dense vegetation concealing entrances, safety issues, or because the caves must be breached in order to enter and survey them. The methodology used for determining cave orientations was subjective and depended on the accuracy of the cave survey and the parameters used to determine orientations, especially in mixing zone caves that are globular or elliptical. The segment lengths that were used in comparisons had the potential of introducing error using the Kolmogorov-Smirnov 2-sample test (Nelson, 1988; Barlow and Ogden, 1992), therefore two sets of segment data were used for all orientation categories. Data types were only considered to be similar if they showed similarity amongst all segment lengths for those data pairs being compared. The degree of breaching may have biased the data, where collapse, cliff retreat or coastal erosion removed portions of the original cave, leaving an incomplete remnant. If a flank margin cave were modeled as a simple ellipse or if flank margin caves are linear features developed parallel to the cliff, then removal of one half or more of the feature by erosion would make the entrance width and the maximum width of the feature the same. In many cases, it appears that at least 50% of the original flank-margin caves had been removed by cliff retreat (Figure 16). The cell size of the DEM limited the resolution of scarps and coastlines. The measurement of fracture orientations in the field was subject to human error, as were the faults and joints reported by Doan and coworkers (1960), which were based on interpretation of data gathered during fieldwork conducted in the 1950's. All of these biases may have affected the comparison of independent data populations, therefore only data pairs that showed a high degree of similarity ($P \leq 0.01$) were considered to be related.

Comparisons between orientations of brittle failure features, scarp and coastline orientations, and cave primary and segment orientations show a wide range of orientation trends at the island and province scale, but more distinct trends at smaller-scale test sites. This wide range of variability at the larger scales may be the result of the physiographic nature of islands. Coastline and scarp orientation trend datasets show a wide range of orientation trends at large region or entire island scales because of the roughly elliptical shape of islands. Island coastlines have orientation trends between 0^o and 360^o because islands are surrounded on all sides by water, therefore a wide range of orientations exist for coastline orientations at the island scale. Similarly, any ridge that may produce scarps will be roughly elliptical in shape and also show a wide range of orientations. However, trend orientations associated with the long axis of these features will show greater dominance as the length to width ratio increases ($L/W > 1$) for the island and scarps (Figure 17).

The orientations of brittle deformation structures reported by Doan and coworkers

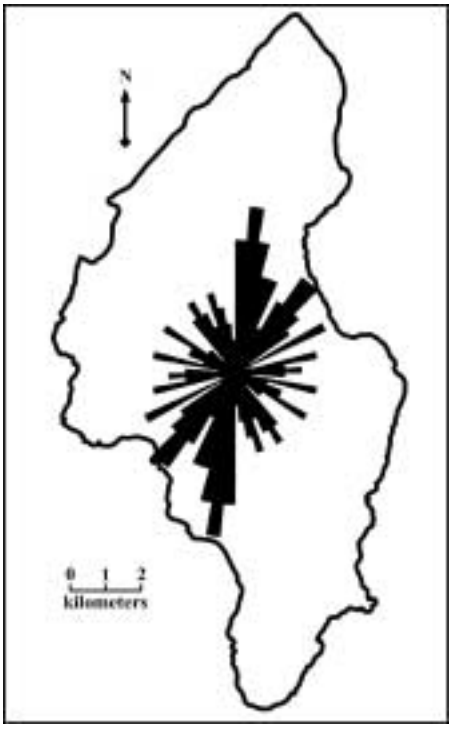

Figure 17: Coastline orientations for Tinian show a wide range of trends because of the elliptical shape of the island. Note that the rose diagram pattern for coastlines resembles the coast outline of Tinian.

(1960) and those measured during fieldwork show a wide range of trends. This is probably the result of Tinian's complex tectonic setting. Tinian is a Paleogene volcanic edifice mantled by younger carbonate rocks with complex, high-angle normal faulting throughout the island. The geomorphology of Tinian is primarily controlled by three factors: 1) the original volcanic depositional regime, 2) the original carbonate depositional regime, and 3) structural deformation primarily in the form of brittle failure. The coastlines of Tinian are primarily erosional, with modern carbonate beach deposits representing less than 5% of the coastline (light blue regions in Figure 39, Appendix A), and strongly influenced by geologic structure. Because of the erosional nature of the coastline and the geomorphology of Tinian, three types of brittle failure are expected to exist (Figure 38): 1) regional faulting associated with island arc tectonism, 2) brittle failure near-parallel to coastlines associated with margin failures, and 3) brittle failure near-perpendicular to coastlines associated with tension release structures that form perpendicular to margin failures (Doan et al., 1960). In addition to the three primary types of brittle failure expected, rock units may also be fractured by passive, isostatic subsidence (>0.05 mm/yr, Dickinson, 1999). The combination of the faulting and fracturing from subsidence and margin failure creates great variability in the orientations of brittle failure features observed on Tinian.

ISLAND SCALE COMPARISONS

At the island scale, comparisons showed 60% similarity in paired, independent samples. This high degree of similarity appears to indicate that the complex nature of brittle deformation and the great variability of coastline and scarp orientations make it impossible to differentiate between relationships at the island scale. The similarity also does not enable the elimination of variables that may not be influencing cave and karst development, because scarps, coastlines, brittle failure features and cave development all show similarities indicating that at large scales the interaction of these variables is too complex to define cause and affect. However, rose diagrams show that, at the island scale, scarps are the only features that show similarity to cave development, suggesting that cave development is primarily controlled by the position of the fresh-water lens if the scarps do represent paleo-coastlines, as predicted in the Carbonate Island Karst Model (Stafford et al., 2003; Jenson et al., 2002; Mylroie and Jenson, 2002; Mylroie and Jenson, 2001).

PROVINCE SCALE COMPARISONS

At the physiographic province scale, fewer independent pairs showed similarity; however, rose diagrams showed more similar pairs. Data for the Northern Lowland and North-Central Highland showed the least degree of similarity in comparisons, which is probably due to a sampling bias of cave and karst features. Only two features were located in the Northern Lowland (one fissure cave and one mixing zone cave) and eight mixing zone caves were located in the North-Central Highland. Therefore, these small sample sizes suggest that these regions do not have enough data to be analyzed with any confidence. The other physiographic provinces produced larger datasets and appeared to have less sampling bias.

The cave inventory of the Central Plateau surveyed 5 fissure caves and 46 mixing zone caves. Rose diagrams show no distinct similarities amongst independent orientation populations. However, statistical analysis of the data showed significant similarity in 45% of the independent sample pairs. Analysis of the data showed similarity between faults, scarps, coastlines, fissure caves and mixing zone caves. This presents the same problem as the island-scale analyses. The Central Plateau, which extends from the east coast to the west coast, exhibited too much variability in the data to determine if brittle failure features,

coastlines or scarps were the dominant control on cave development. The data for the Central Plateau suggests that brittle failure does significantly influence cave development in the region. In the Central Plateau similarity with caves to scarps and coastlines (paleo and modern fresh-water lens) appeared to dominate in all cases except fissure caves, which only showed significant similarity to faults.

The cave inventory of the Median Valley surveyed 5 fissure caves and 27 mixing zone caves. Rose diagrams showed similarities between fractures, scarps, and mixing zone cave entrance widths, suggesting that the breaching of mixing zone caves is associated with scarp failure as expected. Statistical analysis of data showed significant similarity for 43% of the independent data pairs, with similarity between faults, scarps, coastlines and cave development. The only statistical similarity seen for fissure caves was with coastlines. The Median Valley, which extends from the east coast to the west coast, again showed too much variability in the data to determine if brittle failure features, coastlines or scarps were the dominant control on cave development. The similarity between fissure caves segments and coastlines, suggests that the fissure caves in this region are associated with bank-margin failure and not regional faulting; however, the segment data is being highly biased towards one cave (Dripping Tree Fracture Cave) that is significantly longer than the other fissure caves combined.

Seven fissure caves and forty-six mixing zone caves were inventoried on the Southeastern Ridge. Rose diagrams showed more distinct similarities in this province than in others. Fault orientations appeared similar to mixing zone primary orientations and penetrations, while scarps and coastlines showed similarity to mixing zone cave widths. Statistical analysis showed similarities for 53% of the independent data pairs, with similarity between faults, scarps, coastlines and cave development. As in the Central Plateau and Median Valley, the data showed too much variability to determine the dominant control on cave development. However, the data for the Southeastern Ridge suggests that the fissure caves in this region are associated with scarp failures, while mixing zone caves are controlled by a combination of fault and fresh-water lens position. Mixing zone cave penetration shows significant similarity to faults, while mixing zone cave widths are significantly similar to scarps and coastlines. This suggests that mixing zone dissolution at the edge of the fresh-water lens expanded laterally in relation to the edge of the lens and inland in relation to regional fault patterns.

SMALL-SCALE TEST SITE COMPARISONS

The one square kilometer test sites showed a lesser degree of orientation variability than was observed in the larger-scale comparisons. Because these were only test sites used to evaluate whether or not orientation similarities exist at different scales on the island, no rose diagrams were used. Instead, analyses were limited to statistical comparisons. The three test sites chosen for small-scale analyses all contained fissure caves, mixing zone caves, faults, and coastline, and were locations where fractures had been measured in the field.

The Carolinas Limestone Forest test site contained three fissure caves and one mixing zone cave. Data analyses showed similarities for 19% of the independent data pairs. Fractures measured in the field showed significant similarity to regional faults. Segment analyses only showed significant similarity for all segment lengths in three data pairs. The significantly similar segment orientations were all related to regional faults and caves, with faults being similar to fissure caves, mixing zone cave maximum widths and all cave type orientations. This data suggests regional faulting controls fissure caves in this area. The similarities between all cave types and mixing zone caves are not considered reliable because of the small sampling size

of mixing zone caves for this regions, but the do suggest that regional brittle deformation may be affecting mixing zone development.

The Puntan Diapblo test site contained three fissure caves and nine mixing zone caves. Data analyses showed similarities for 16% of the independent data pairs. Fractures measured in the field showed similarity to faults, scarps, fissure caves and mixing zone cave widths. As in the Carolinas Limestone Forest test site, similarity between segment orientations were only seen in relation to faults. Faults were similar to inland scarps and mixing zone cave penetrations, suggesting regional jointing and faulting influence mixing zone cave development. The lack of similarity between faults and the fissure cave development does not mean that these fissure caves are not controlled by brittle deformation. Similarity seen between fractures measured in the field and the fissure caves suggests that these fissure caves are controlled by fractures that are near perpendicular to the coastline and may be related to unloading structures associated with regional isostatic subsidence or tension release features.

The Unai Dangkolo test site contains one fissure cave and five mixing zone caves. Data analyses showed similarities for 45% of the independent data pairs, which appears high. Data for this test site was limited because analyses of the DEM showed that no major scarps exist in this area. Fractures measured during fieldwork and faults both showed similarity to the coastline and mixing zone cave development. Coastline orientations showed similarity to fissure caves and mixing zone caves. This data suggests that mixing zone caves in this area are influenced by both the coastline (edge of the fresh-water lens) and regional faulting. Fissure cave development appears to be completely associated with coastlines, suggesting that Dripping Tree Fracture cave is related to bank-margin failure parallel to the coastline.

STRUCTURAL CONTROL OF CAVES

Eogenetic karst development on Tinian is dominated by mixing zone dissolution; however, brittle deformation appears to have a significant influence. Seventy-seven percent of the caves surveyed on Tinian are mixing zone caves, while only twenty percent are fissure caves. These two groups of caves are significantly different and their developmental controls are different.

Orientations of fissure caves showed significant similarity to zones of brittle failure; however, the type of brittle failure is varied. Independently, orientations of fissure caves show similarities to regional faulting, jointing, coastline and scarp position. The statistical comparisons imply that fissure cave development is controlled by brittle failure that results from island tectonism (high-angle faulting), passive isostatic subsidence (joints), and scarp failure (fractures). Additionally, most fresh-water discharge observed on Tinian was associated with fissure caves or smaller-scale dissolutionally widened bedrock fractures.

Mixing zone caves appear to be primarily controlled by the fresh-water lens position; however, orientation similarities between mixing zone caves and brittle deformation features exist in analyses ranging from the small-scale test areas to the entire island of Tinian. Although the relationships are not consistent from region to region, analyses of the orientation data suggest that brittle deformation does significantly affect mixing zone development.

KARST DEVELOPMENT ON AGUIJAN AND TINIAN

This study indicates that karst development on Tinian is dominated by mixing zone dissolution, but that geologic structure, in the form of brittle deformation, plays a significant role. Significant similarities between independent populations or population distributions confirm that the structural controls on fissure cave development inferred from cave

morphology are correct and that mixing zone caves are being significantly influenced by brittle failure. Based on the presence of at least three zones of mixing zone cave development, it is believed that Tinian and Aguijan have experienced several stable sea-level stillstands that lasted for significant periods. These horizons probably represent previous sea-level stillstands related to glacio-eustacy with constant uplift; however, they may indicate episodic island uplift. Some flank-margin caves are vertically exaggerated; suggesting slow uplift, slow sea level change or a combination of the two at times.

The data indicate that Tinian does not conveniently fit in to any single model for carbonate island karst. The data do not suggest that Tinian is a Complex Carbonate Island because no intricate interfingering of carbonate and non-carbonate facies were identified, although the island does show a high degree of faulting. The high-angle faulting does appear to separate the island into distinct regions and significantly distort the fresh-water lens as indicated by fresh-water discharge sites identified near the boundaries between the Median Valley and Southeastern Ridge and between the Northern Lowland and Central Plateau. The Northern Lowland best fits the Simple Carbonate Island Karst Model, with fresh-water exposed at the surface at Hagoi and no non-carbonate rocks cropping out. The Southeastern Ridge best fits the Carbonate-Cover Island Karst Model, with several areas of mixing zone cave development and non-carbonate rocks that outcrop, but do not show any direct evidence of allogenic recharge. The Central Plateau, North-Central Highland and Median Valley cannot be easily fit into separate models, but together best fit the Composite Island Karst Model with allogenic recharge occurring at the non-carbonate / carbonate rock contacts in the North-Central Highland. Because the central portion of the Tinian best fits the Composite Island Karst Model, the entire island must be classified as this although the northern and southern portions of the island do not represent this model well.

Aguijan can only be classified as a Simple Carbonate Island because only carbonate rocks are known. However, the geomorphology of Aguijan is similar to that of the Southeastern Ridge of Tinian, indicating that it is most likely a Carbonate-Cover Island. Further complicating the interpretation of Aguijan is Liyang Atkiya, which may indicate some complex interaction between carbonate and non-carbonate rocks.

SUMMARY

This study inventoried and surveyed 26 cave and karst features on Aguijan and 88 cave and karst features on Tinian and is believed to have adequately sampled the cave and karst development on the islands, although it is probable that more features exist. Two distinct classes of cave and karst features were identified: mixing zone caves (flank margin and banana hole type caves) and fissure caves (linear caves associated with planes of brittle failure). Most mixing zone caves are located in or near scarps and coastlines, at elevations from sea level to 160 meters, have areas from a few square meters to more than 1300 square meters, and are often at consistent levels with nearby caves. At least three distinct horizons of breached mixing zone caves occur on Tinian, representing previous fresh-water lens positions that have been tectonically uplifted and breached by erosional processes. Fissure caves were located in regions that showed evidence of brittle failure produced from active tectonic uplift, passive isostatic subsidence, or bank margin and smaller scale scarp failure. The fissure caves range in length from a few tens of meters to hundreds of meters and are

relatively narrow. Some of these features reached significant depth. The fissure caves show direct evidence of vadose fast flow routes, which can rapidly transmit fluids more than 40 meters into the subsurface and can distort the fresh-water lens morphology. Although some fissure caves extended over longer distances and to greater depths than the mixing zone caves, mixing zone caves were found to be significantly more abundant (mixing zone cave / fissure caves = 4).

In addition to the karst inventory, fresh-water discharge and allogenic recharge sites were investigated. Along the coastline of Tinian, 17 fresh-water discharge sites were identified, many associated with sea level caves. No active discharge sites were identified on Aguijan because strong surf conditions prevented exploration, but two paleo-discharge sites were identified on the Middle Terrace. Four closed depressions were identified as sites of allogenic recharge on Tinian at contacts between non-carbonate igneous outcrops and carbonate rocks, including two with caves that receive direct recharge. No allogenic recharge sites were identified on Aguijan because only carbonate rocks outcrop on the island.

Orientation data showed that brittle failure features significantly influence karst development on Tinian. At the island scale and regional scale, it is difficult to determine if megaporosity (cave) development is associated with geologic structure or with fresh-water lens position (scarps and coastlines), because of the wide range of data orientations on Tinian, resulting from the island geomorphology and complex tectonic setting. However, similarities between data populations or population distributions suggest that geologic structure does affect karst development. At smaller scales, more direct evidence of structural controls on megaporosity development are seen, probably resulting from the narrower range of orientation data present at these scales because of smaller sample sizes.

Analyses of cave maps in relation to brittle failure and island geomorphology indicates that the interpretations for origin of fissure caves that have been inferred from cave morphology are correct. Fissure cave orientation trends in the vicinity of faulting show significant similarity to faults, implying that the caves formed along preferential flow paths created by faulting. Fissure cave orientation trends near coastlines and scarps show significant similarities to nearby fractures, implying that the caves formed along preferential flow paths created by bank-margin and smaller-scale scarp failure or in relation to tension release structures. Orientations of mixing zone caves show significant similarities to scarps and coastlines, implying that the caves formed in relation to the edge of the fresh-water lens. However, mixing zone caves often show similarities with brittle failure features, suggesting that mixing zone caves are significantly influenced by geologic structure, although mixing zone dissolution along the edge of the fresh-water lens is the dominant controlling factor. Clearly, the interaction between megaporosity development and brittle deformation on carbonate islands is complex, often resulting in features that are primarily controlled by different factors (fresh-water lens position or brittle deformation) developing close to each other (Figure 18).

Tinian and Aguijan show that the Carbonate Island Karst Model cannot be simply applied to entire carbonate islands that occur in complex tectonic settings. In order to apply the Carbonate Island Karst Model to Tinian it must be divided into different regions. The Northern Lowland best fits the Simple Carbonate Island Karst Model. The Southeastern Ridge best fits the Carbonate-Cover Island Karst Model. The North-Central Highland, Central Plateau, and Median Valley cannot be easily separated, but when grouped together best fit the Composite Island Karst Model. Aguijan must be classified as a Simple Carbonate Island because no proof has been found to confirm that the island has a core of non-carbonate rocks that extend above sea

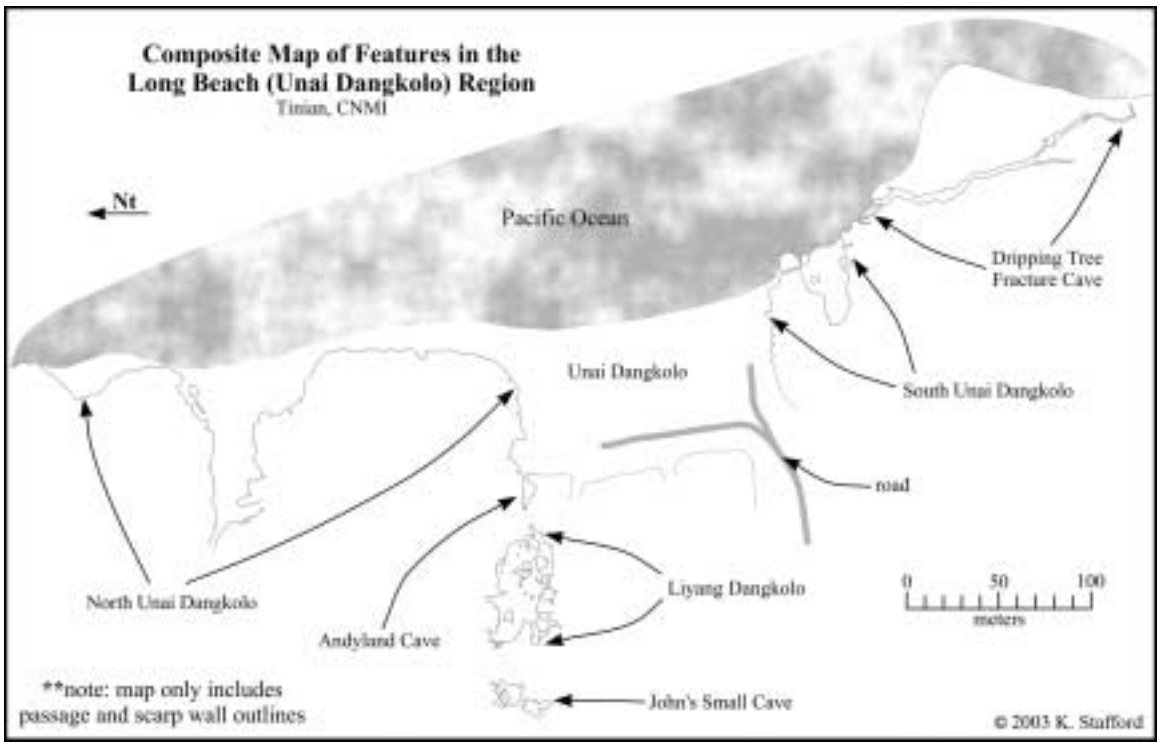

Figure 18: Map of Unai Dangkolo region showing the close proximity of lank margin cave and fissure cave development.

level and partition the fresh-water lens. However, based on Aguijan's similarity with the Southeastern Ridge of Tinian it probably best fits the Carbonate-Cover Island Karst Model.

Geologic investigations on the islands of Tinian and Aguijan have been limited in the past and much remains to be done in future research, which is beyond the scope of this study. The cave and karst inventory surveyed the majority of known cave and karst features on Tinian and Aguijan; however, more features exist which need to be identified and surveyed. Basic geologic mapping is still needed for the island of Aguijan. During this study, the author and other investigators sampled speleothems, paleosols, and cave sediments, which may provide greater insight into the geology and hydrogeology of the Mariana Islands. Future isotope analysis of speleothems and petrographic analysis of paleosols may provide important information about the paleoclimatic history of the region, while future analysis of cave sediments may elucidate the origin of Liyang Atkiya.

REFERENCES CITED

Aby, S.B., 1994. Relation of bank-margin fractures to sea level change, Exuma Islands, Bahamas. Geology, v. 22, pp. 1063-1066

Back, W., Hanshaw, B.B., and Van Driel, J.N., 1984. Chapter 12, Role of groundwater in shaping the Eastern Coastline of the Yucatan Peninsula, Mexico. *in* LaFleur, R.G. (Editor), Groundwater as a Geomorphic Agent, Allen & Unwin, Inc., Boston, pp. 281-293.

Barlow, C.A., and Ogden, A.E., 1992. A statistical comparison of joint, straight cave segment, and photo-lineament orientations. NSS Bulletin, v. 44, pp. 107-110.

Bormann, N.E., 1992. Ground-water resources management on Tinian, CNMI. American Water Resources Association technical publication series, v. 92-1, pp. 35-44.

Burke, H.W., 1953. The Petrography of the Mariana Limestone, Tinian, Mariana Islands. Graduate dissertation, Stanford University, 111 p.

Burt, J.E., and Barber, G.M., 1996. Elementary Statistics for Geographers: Second Edition. The Gulford Press, New York, NY, 640 p.

Butler, B.M, 1992. An Archaeological Survey of Aguiguan (Aguijan), Northern Mariana Islands: Micronesian Archaeological Survey Report Number 29. The Micronesian Archaeological Survey. Division of Historic Preservation, Dept. of Community and Cultural Affairs, Saipan, MP, 260 p.

Carew, J.L., and Mylroie, J.E., 1995. Quaternary tectonic stability of the Bahamian Archipelago: evidence from fossil coral reefs and flank margin caves. Quaternary Science Reviews, v. 14, pp. 145-153.

Cloud, P.E., Jr., Schmidt, R.G., and Burke, H.W., 1956. Geology of Saipan, Mariana Islands, Part 1. General Geology. 280-A, U.S. Geological Survey Professional Paper, U.S. Government Printing Office, Washington, D.C., pp. 126.

Dasher, G.R., 1994. On Station. National Speleological Society, Inc., Huntsville, Alabama, 242 p.

Dickinson, W.R., 1999. Hydro-isostatic and tectonic influences on emergent Holocene paleoshorelines in the Mariana Islands, Western Pacific Ocean. Journal of Coastal Research, v. 16, no. 3, pp. 735-746.

Doan, D.B., Burke, H.W., May, H.G., Stensland, C.H., and Blumenstock, D.I., 1960. Military Geology of Tinian, Mariana Islands. Chief of Engineers, U.S. Army, 149 p.

ESRI, 2000. ArcView GIS 3.2. Environmental Systems Research Institute, Inc., software.

Folk, R.L., Roberts, H.H., and Moore, C.C., 1973. Black phytokarst from Hell, Cayman Islands, British West Indies. Geological Society of America Bulletin, v. 84, pp. 2351-2360.

Frank, E.F., Mylroie, J.E., Troester, J., Alexander, E.C., and Carew, J.L., 1998. Karst development and speleologensis, Isla de Mona, Puerto Rico. Journal of Cave and Karst Studies, v. 60, no. 2, pp. 73-83.

Gingerich, S.B., and Yeatts, D.S., 2000. Ground-Water Resources of Tinian, Commonwealth of the Northern Mariana Islands, Water-resources Investigations Report 00-4068. U.S. Department of the Interior, 2 sheets.

Gross, M.G., 1982. Oceanography: A View of the Earth. Prentice-Hall, Inc., Eaglewood Cliffs, NJ, 498 p.

Harris, J.F., Mylroie, J.E. and Carew, J.L., 1995. Banana holes: Unique karst features of the Bahamas. Carbonates and Evaporites, v. 10, no. 2, pp. 215-224.

Holcombe, R., 2003. GEOrient 9.2. Department of Earth Sciences, University of Queensland, Australia.

http://www.earth.uq.edu.au/~rodh/software/

Hunt, E., and Wheeler, T., 2000. South Pacific. Lonely Planet Publications, Oakland, CA, 928 p.

Jenson, J.W., Jocson, J.M.U., and Siegrist, H.G., 1997. Groundwater discharge styles from an uplifted Pleistocene island karst aquifer, Guam, Mariana Islands. *in* Beck, B.F. and Stephenson, J.B. (Editors), The Engineering Geology of Karst Terraines, Balkema, Springfield, Missouri. pp. 27-32.

Jenson, J.W., Mylroie, J.E., Mylroie, J.R., and Wexel, C., 2002. Revisiting the carbonate island karst model. Geological Society of America Abstracts with Program, v. 34, no. 6, p. 226.

Jocson, J.M.U., Jenson, J.W., and Contractor, D.N., 2002. Recharge and aquifer responses: Northern Guam Lens Aquifer, Guam, Mariana Islands. Journal of Hydrology, v. 260, pp 231-254.

Jocson, J.M.U., Jenson, J.W., and Contractor, D.N., 1999. An Integrated Numerical Modeling Study and Field Investigation of the Northern Guam Lens Aquifer. Technical Report #88, Water and Environmental Research Institute of the Western Pacific, University of Guam, Mangilao, 34 p.

Klimchouk, A., and Ford, D., 2000. Chapter 3.2, Lithologic and structural controls of dissolutional cave development. *in* Klimchouk, A., Ford, D., Palmer, A., and Dreybrodt, W. (Editors), Speleogenesis: Evolution of Karst Aquifers. National Speleological Society, Huntsville, AL, pp. 54-64.

Mink, J.F., and Vacher, H.L., 1997. Hydrogeology of northern Guam. *in* Vacher, H.L., and Quinn, T. (Editors), Geology and Hydrogeology of Carbonate Islands. Developments in Sedimentology 54, Elsevier Science, pp. 743-761.

Miller, R.L., and Kahn, J.S., 1962. Appendix G: The Kolmogorov-Smirnov Statistic. in. Miller, R.L., and Kahn, J.S., Statistical Analysis in the Geological Sciences. John Wiley and Sons, Inc., New York, NY, pp. 464-468.

McClure, G.E., 1977. Tinian, Then and now..: 5th edition. Glenn E. McClure, Universal City, TX, 28 p.

McKenzie, D., 2002. WALLS Project Editor – Beta Version 2.0 B6. http://davidmck.home.texas.net/walls/, shareware software.

Mylroie, J.E., and Carew, J.L., 1997. Land use and carbonate island karst. *in* Beck and Stephenson (Editors), The Engineering and Hydrology of Karst Terranes. Balkema, Rotterdam, pp. 3-12.

Mylroie, J.E., and Carew, J.L., 1995a. Karst development on carbonate islands. *in* Budd, D.A., Harris, P.M., and Staller, A. (Editors), Unconformities and Porosity in Carbonate Strata. American Association of Petroleum Geologists, pp. 55-76.

Mylroie, J.E., and Carew, J.L., 1995b. Geology and karst geomorphology on San Salvador Island, Bahamas. Carbonates and Evaporites, v. 10, no. 2, pp. 193-206.

Mylroie, J.E., and Carew, J.L., 1991. Erosional notches in Bahamian carbonates: bioerosion or groundwater dissolution?. *in* Bain, R.J. (Editor), Proceedings of the Fifth Symposium on the Geology of the Bahamas. Bahamian Field Station, San Salvador, Bahamas, pp. 185-191.

Mylroie, J.E., Carew, J.L., and Vacher, H.L., 1995a. Karst development in the Bahamas and Bermuda. In: Curran, H.A., and White, B. (Editors), Terrestrial and Shallow Marine Geology of the Bahamas and Bermuda, pp. 251-267.

Mylroie, J.E., Carew, J.L., and Moore, A.I., 1995c. Blue hole: definition and genesis. Carbonates and Evaporites, v. 10, no. 2, pp. 225-233.

Mylroie, J.E., and Jenson, J.W., 2002. Karst flow systems in young carbonate islands. *in* Martin, J.B., Wicks, C.M.,

and Sasowsky, I.D. (editors), Hydrogeology and biology of post-Paleozoic carbonate aquifers. Karst Waters Institute Special Publication Number 7, Karst Waters Institute, Inc., Charles Town, WV, pp. 107-110.

Mylroie, J.E., and Jenson, J.W., 2001. The carbonate island karst model applied to Guam. Theoretical and Applied Karstology, v. 13-14, pp. 51-56.

Mylroie, J.E., Jenson, J.W., Jocson, J.M.U., and Lander, M., 1999. Karst Geology and Hydrology of Guam: A Preliminary Report, Technical Report #89. Water and Environmental Institute of the Western Pacific, University of Guam, Mangilao, 32 p.

Mylroie, J.E., Jenson, J.W., Taborosi, D., Jocson, J.M.U., Vann, D., and Wexel, C., 2001. Karst features of Guam in terms of a general model of carbonate island karst. Journal of Cave and Karst Studies, v. 63, no. 1, pp. 9-22.

Mylroie, J.E., Panuska, B.C., Carew, J.L., Frank, E., Taggart, B.E., Troester, J.W., and Carrasquillo, R., 1995b. Development of flank margin caves on San Salvador Island, Bahamas and Isla de Mona, Puerto Rico. *in* Boardman, M. (Editor), Proceedings of the Seventh Symposium on the Geology of the Bahamas. Bahamian Field Station, San Salvador, Bahamas, pp. 49-81.

Mylroie, J. E., and Vacher, H. L., 1999. A conceptual view of carbonate island karst. *in* Palmer, A. N., Palmer, M. V., and Sasowsky, I. D. (Editors), Karst Modeling, Karst Waters Institute Special Publication 5, Karst Waters Institute, Inc., Charles Town, WV, pp. 48-57.

Nelson, J.W., 1988. Structural and Geomorphic Controls of the Karst Hydrogeology of Franklin County, Alabama [MS Thesis]. Mississippi State University, 165 p.

Palmer, A.N., 1991. Origin and morphology of limestone caves. Geological Society of America Bulletin, v. 103, pp. 1-21.

Raeisi, E., and Mylroie, J.E., 1995. Hydrodynamic behavior of caves formed in the fresh-water lens of carbonate islands. Carbonates and Evaporites, v. 10, no. 2, pp. 207-214

Reagan, M.K., and Meijer, A., 1984. Geology and geochemistry of early arc-volcanic rocks from Guam. Geological Society of America Bulletin, v. 95, pp. 701-713.

Sasowsky, I.D., and White, W.B., 1994. The role of stress release fracturing in the development of cavernous porosity in carbonate aquifers. Water Resources Research, v. 30, no. 12, pp. 3523-3530.

Siegrest, H.G., 1988. Miocene reef carbonates of the Mariana Islands. American Association of Petroleum Geologists Bulletin, v. 72, no. 2, p. 248.

Sprouse, P., 1991. Proyecto Espeleologico Purificacion: Standard cave map symbols. The Death Coral Caver, no. 2, p. 37.

Sprouse, P., and Russell, W., 1980. AMCS cave map symbols: AMCS Activities Newsletter, no. 11, pp. 64-67.

Stafford, K.W., Mylroie, J.E., Mylroie, J.R., and Jenson, J.W., 2003. Tinian, CNMI: A carbonate island karst model evaluation. Geological Society of America abstracts with programs, v. 35, no. 1, p. 54.

Stafford, K.W., Mylroie, J.E., and Jenson, J.W., 2002. Karst Geology and Hydrology of Tinian and Rota (Luta), CNMI: Technical Report No. 96. Water and Environmental Institute of the Western Pacific, University of Guam, Mangilao, 31 p.

Stafford, K.W., Mylroie, J.E., Mylroie, J.R., and Jenson, J.W., 2003. Tinian, CNMI: A carbonate island karst model evaluation. Geological Society of America Abstracts and Programs, v. 35, no. 1, p. 3.

Sugiwara, S., 1934. Topography, Geology, and Coral Reefs of Rota Island. Pacific Geological Surveys, Military Branch, United States Geological Survey, 59 p.

Taborosi, D.S., 2000. Karst Features of Guam [MS thesis]. University of Guam, Mangilao, 19 p.

Taborosi, D.S., and Jenson, J.W., 2002. World War II artefacts and wartime use of caves in Guam, Marian Islands. Capra 4, http://www.shef.ac.uk/~capra/4/.

Taborosi, D., Jenson, J.W., and Mylroie, J.E., in press. Karren features in island karst: Guam, Mariana Islands. Zeitschrift fur Geomorphologie.Tayama, R., 1936. Geomorphology, Geology, and Coral Reefs of Tinian Island Together with Aguijan and Naftan Islands. Institute of Geology and Paleontology, Tohoku University, Japan. 72 p.

Till, R., 1974. Chapter 7: Non-Parametric Statistics. in Till, R., Statistical Methods for the Earth Scientist. John Wiley and Sons, Inc., New York, NY, pp. 117-138.

Twiss, R.J., and Moores, E.M., 1992. Structural Geology. W.H. Freeman and Company, U.S., 532 p.

Tracey, J.I., Jr., Schlanger, S.O., Stark, J.T., Doan, D.B., and May, H.G., 1964. General Geology of Guam. 403-A, U.S. Geological Survey Professional Paper, U.S. Government Printing Office, Washington, D.C., 104 p.

United States Department of the Interior Geological Survey, 2001a. 1697184.DEM.SDTS.TAR.GZ. National Mapping program of the U.S. Geological Survey, ftp://sdts.er.usgs.gov/pub/sdts/datasets/raster/dem/

United States Department of the Interior Geological Survey, 2001b. 1697335.DEM.SDTS.TAR.GZ. National Mapping program of the U.S. Geological Survey, ftp://sdts.er.usgs.gov/pub/sdts/datasets/raster/dem/

United States Department of the Interior Geological Survey, 2001c. 1697336.DEM.SDTS.TAR.GZ. National Mapping program of the U.S. Geological Survey, ftp://sdts.er.usgs.gov/pub/sdts/datasets/raster/dem/

United States Department of the Interior Geological Survey, 2001d. 1697337.DEM.SDTS.TAR.GZ. National Mapping program of the U.S. Geological Survey, ftp://sdts.er.usgs.gov/pub/sdts/datasets/raster/dem/

United States Department of the Interior Geological Survey, 2001e. 1697338.DEM.SDTS.TAR.GZ. National Mapping program of the U.S. Geological Survey, ftp://sdts.er.usgs.gov/pub/sdts/datasets/raster/dem/

United States Department of the Interior Geological Survey, 1983. Topographic Map of the Island of Tinian, Commonwealth of the Northern Mariana Islands: U.S. Geological Survey, scale 1:25,000.

Vacher, H.L., and Mylroie, J.E., 2002. Eogenetic karst from the perspective of an equivalent porous medium. Carbonates and Evaporites, v. 17, no. 2, pp. 182-196.

Viles, H. A., 1988. Biogeomorphology. Basil Blackwell, Oxford, United Kingdom, 325 p.

White, W.B., 1988. Geomorphology and Hydrology of Karst Terrains. Oxford University Press, New York, 464 p.

Xara, 1997. CorelXara 2.0. Xara Ltd., Hertfordshire, United Kingdom, http://www.xara.com, software.